



The mini-review of lower Sigma($1/2^-$) around 1400 MeV

Jia-Jun Wu (UCAS)

ROCKSTAR: TOWARDS A ROADMAP OF THE CRUCIAL MEASUREMENTS OF KEY OBSERVABLES IN STRANGENESS REACTIONS FOR NEUTRON STARS EQUATION OF STATE

2023. 10. 13.

ECT* (Trento, Italy)



Outline

- Background
- Theoretical predictions
- Experimental searching
- Summary and Outlook

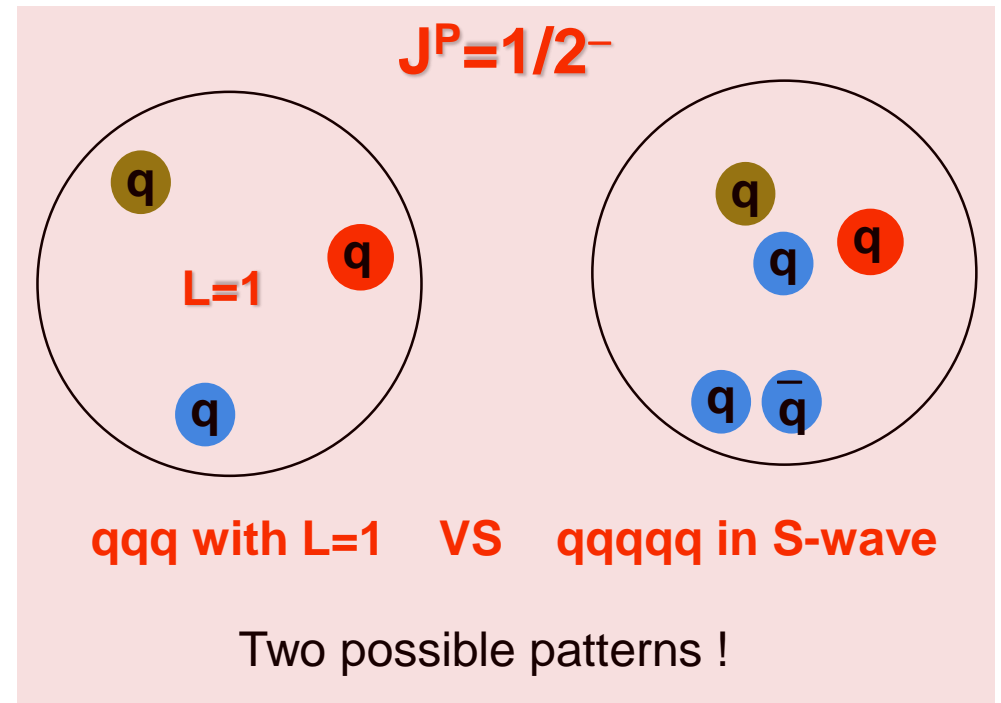
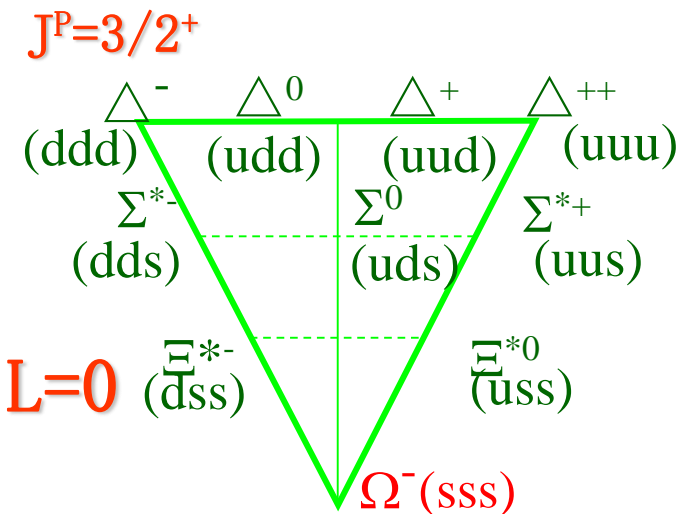
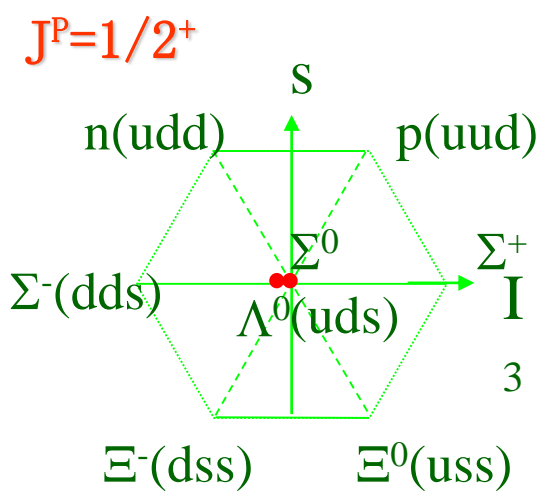


中国科学院大学
University of Chinese Academy of Sciences



Background

- Three quark model



Excited state $L=1, J^P=1/2^-$

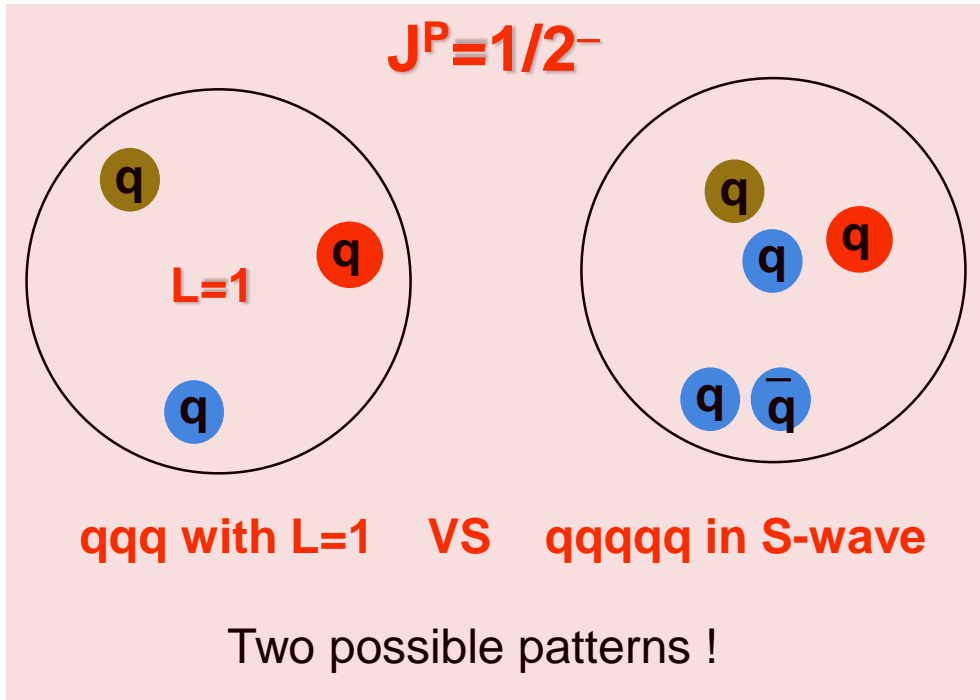
$N^*(1535), \Sigma^*(1620), \Lambda^*(1405), \Xi^*(1690?)$

$N(940), \Sigma(1189), \Lambda(1115), \Xi(1314)$

Something Wrong for the 3q model !



Background



VOLUME 2, NUMBER 10

PHYSICAL REVIEW LETTERS

MAY 15, 1959

POSSIBLE RESONANT STATE IN PION-HYPERON SCATTERING*

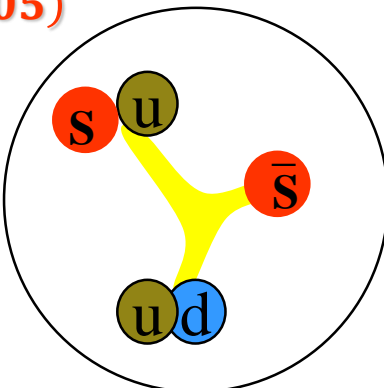
R. H. Dalitz and S. F. Tuan

Enrico Fermi Institute for Nuclear Studies and Department of Physics,
University of Chicago, Chicago, Illinois
(Received April 27, 1959)



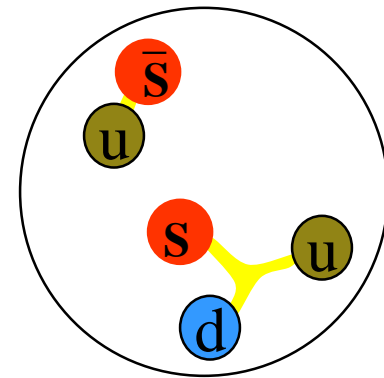
中国科学院大学
University of Chinese Academy of Sciences

$\Lambda^*(1405)$



penta-quark

C. Helminen and D. O. Riska,
NPA699, 624(2002).
S. L. Zhu, etc. High Energy
Phys. Nucl. Phys. 29, 250(2005).
B. S. Zou, EPJA35, 325 (2008).



meson cloud/molecule

N. Kaiser, P. B. Siegel, and W. Weise, PLB 362, 23 (1995).
D. Jido, J. A. Oller, E. Oset, A. Ramos, and U. G. Meissner,
NPA725, 181 (2003).

Theoretical predictions

penta-quark

S. L. Zhu, etc. High Energy Phys.
Nucl. Phys. 29, 250(2005).

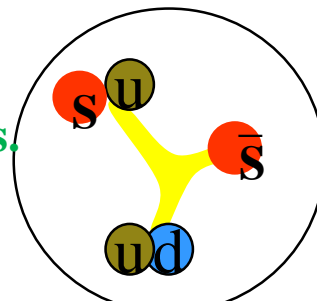
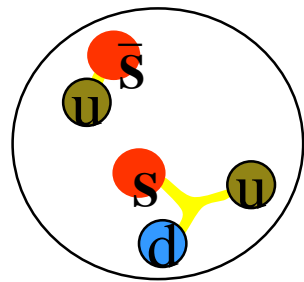
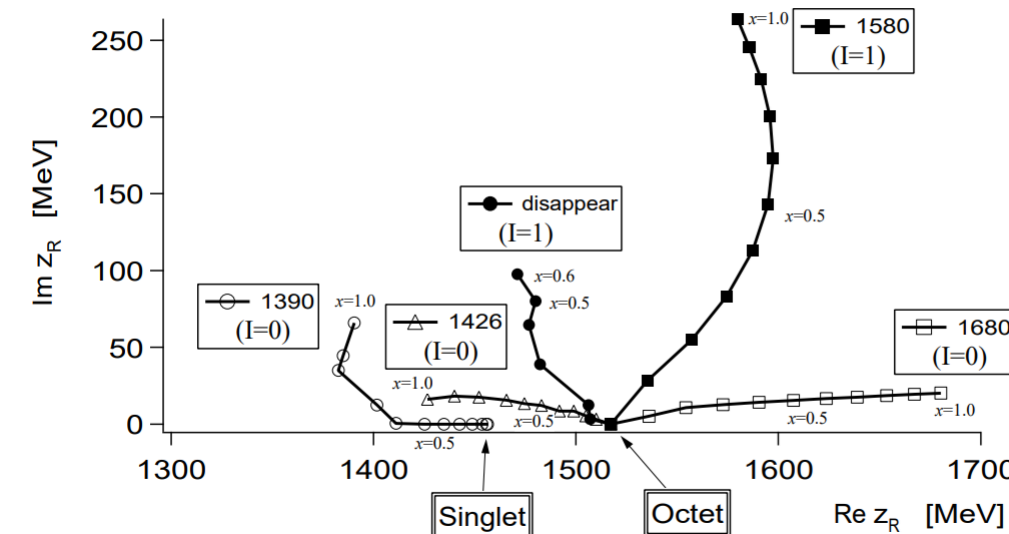


Table 2. Flavor wave functions and masses of the $\frac{1}{2}^-$ pentaquark octet and singlet

	(Y, I)	I_3	flavor wave functions	masses (MeV)
p_8	$(1, \frac{1}{2})$	$\frac{1}{2}$	$[su][ud]_{-\bar{s}}$	1460
n_8		$-\frac{1}{2}$	$[ds][ud]_{-\bar{s}}$	1460
Σ_8^+	$(0, 1)$	1	$[su][ud]_{-\bar{d}}$	1360
Σ_8^0		0	$\frac{1}{\sqrt{2}}([su][ud]_{-\bar{u}} + [ds][ud]_{-\bar{d}})$	1360
Σ_8^-		-1	$[ds][ud]_{-\bar{u}}$	1360
Λ_8	$(0, 0)$	0	$\frac{[ud][su]_{-\bar{u}} + [ds][ud]_{-\bar{d}} - [su][ds]_{-\bar{s}}}{\sqrt{6}}$	1533
Ξ_8^0	$(-1, \frac{1}{2})$	$\frac{1}{2}$	$[ds][su]_{-\bar{d}}$	1520
Ξ_8^-		$-\frac{1}{2}$	$[ds][su]_{-\bar{u}}$	1520
Λ_1	$(0, 0)$	0	$\frac{[ud][su]_{-\bar{u}} + [ds][ud]_{-\bar{d}} + [su][ds]_{-\bar{s}}}{\sqrt{3}}$	1447

meson cloud/molecule

D. Jido, J. A. Oller, E. Oset, A. Ramos, and U. G. Meissner, NPA725, 181 (2003).



Pole	C_1	C_{8_a}/C_1	C_{8_s}/C_1	$ C_1 ^2$	$ C_{8_a} ^2$	$ C_{8_s} ^2$	Pole	C_8	C_{8_s}/C_8	$ C_8 ^2$	$ C_{8_s} ^2$
$1379 + 27i$	0.96	(0.15, 0.11)	(0.15, -0.19)	0.92	0.03	0.05	$1401 + 40i$	0.81	(0.72, 0.07)	0.66	0.34
$1434 + 11i$	0.49	(0.64, 0.77)	(0.71, 1.28)	0.24	0.24	0.52	$1488 + 114i$	0.59	(1.37, -0.06)	0.35	0.65
$1692 + 14i$	0.48	(1.58, 0.37)	(0.78, 0.16)	0.23	0.63	0.14					

J. A. Oller and U.-G. Meißner, Phys. Lett. B 500 (2001) 263



Searching lowlying $\Sigma(1/2^-)$ around 1400MeV

Some evidence

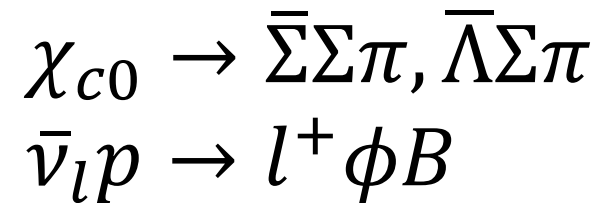
$K^- p$ reaction

γN reaction

Λ_c^+ decay



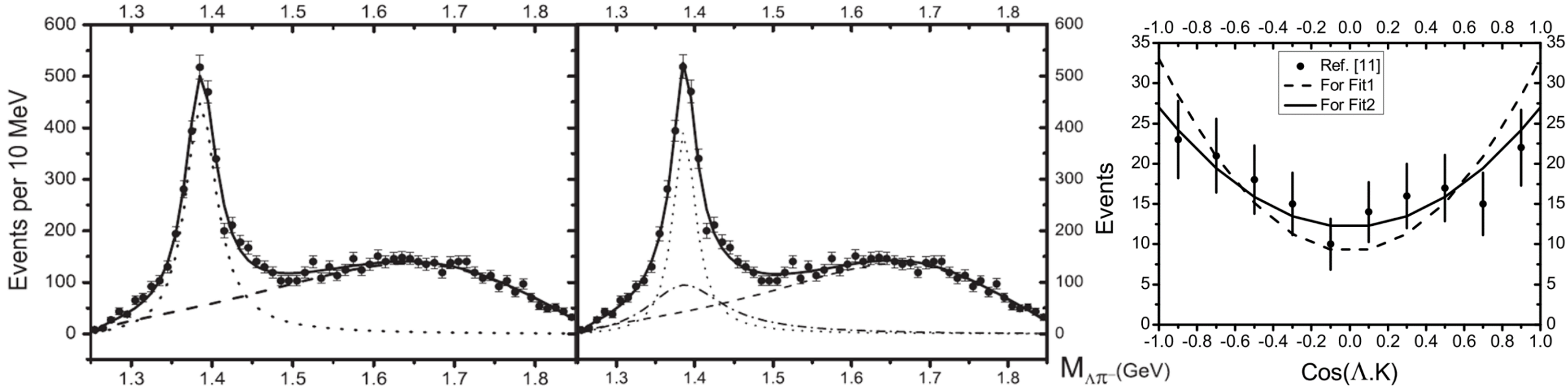
Just prediction



$K^- p \rightarrow \Lambda \pi^+ \pi^-$

$P_K = 1.0 - 1.8 \text{ GeV}$

J. J. Wu, S. Dulat and B. S. Zou PRD 80 (2009), 017503



	$M_{\Sigma^*(3/2)}$	$\Gamma_{\Sigma^*(3/2)}$	$M_{\Sigma^*(1/2)}$	$\Gamma_{\Sigma^*(1/2)}$	χ^2/ndf
Fit1	1385.3 ± 0.7	46.9 ± 2.5			68.5/54
Fit2	$1386.1^{+1.1}_{-0.9}$	$34.9^{+5.1}_{-4.9}$	$1381.3^{+4.9}_{-8.3}$	$118.6^{+55.2}_{-35.1}$	58.0/51

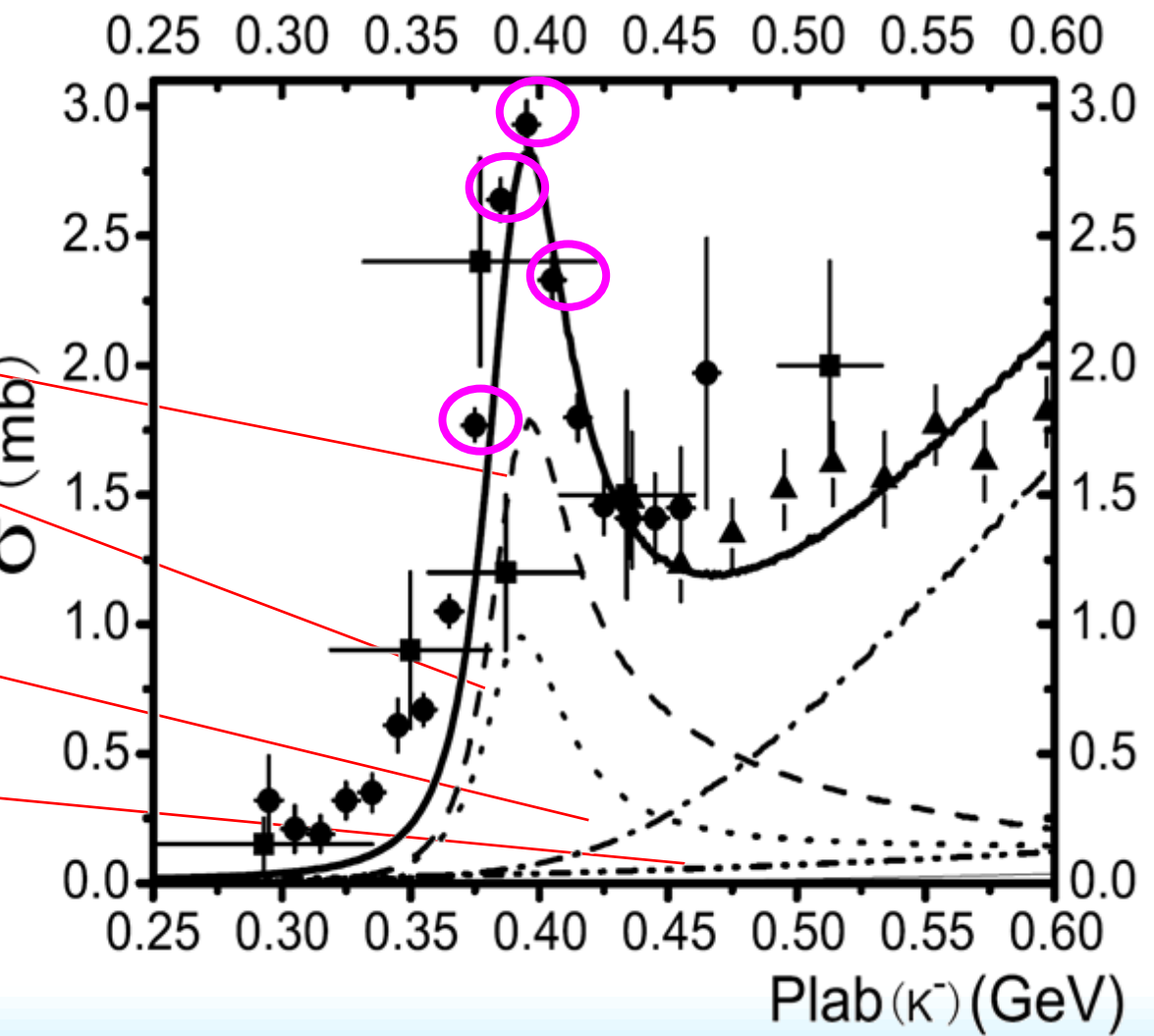
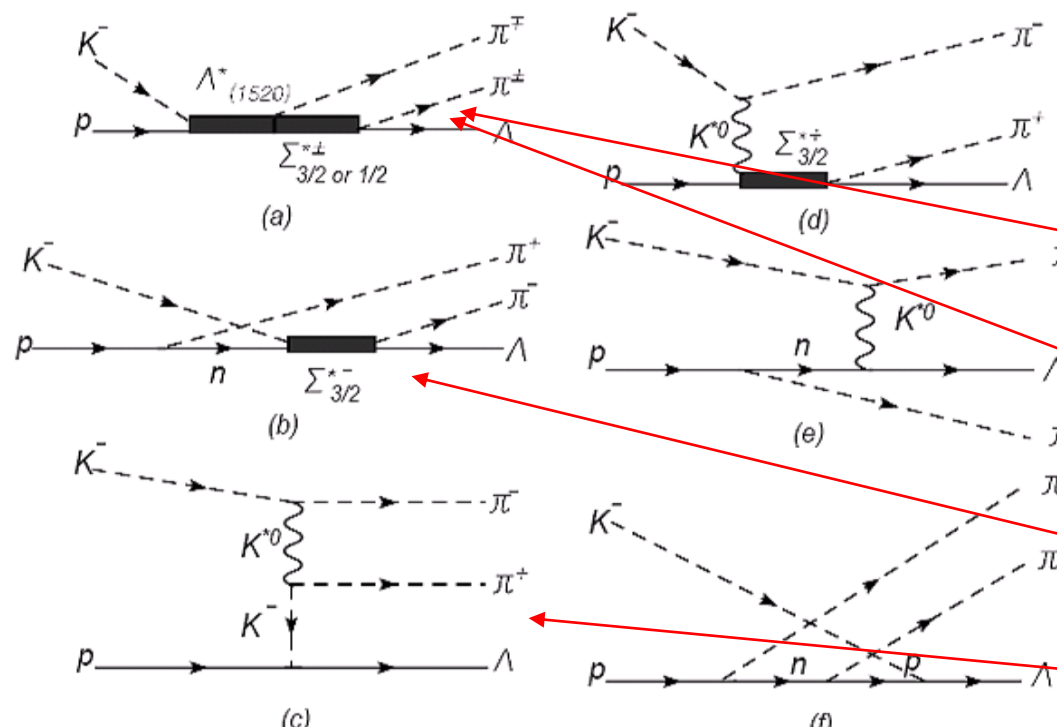
Although the evidence is weak, but the experimental data can not exclude the existence of $\Sigma^*(1/2^-)$



$K^- p \rightarrow \Lambda \pi^+ \pi^-$

$P_K = 0.3\text{--}0.6 \text{ GeV}$

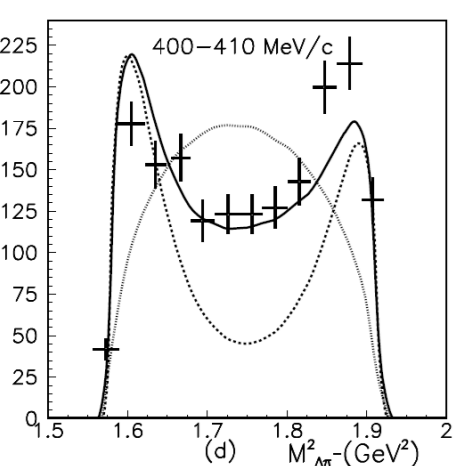
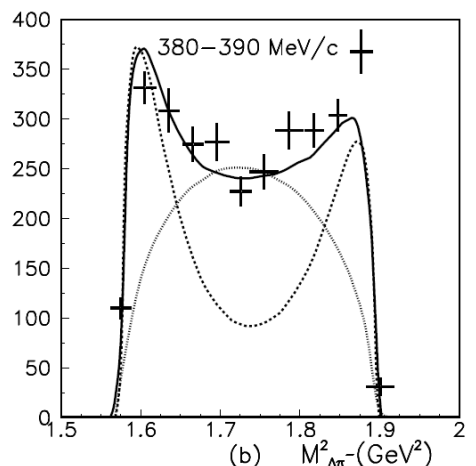
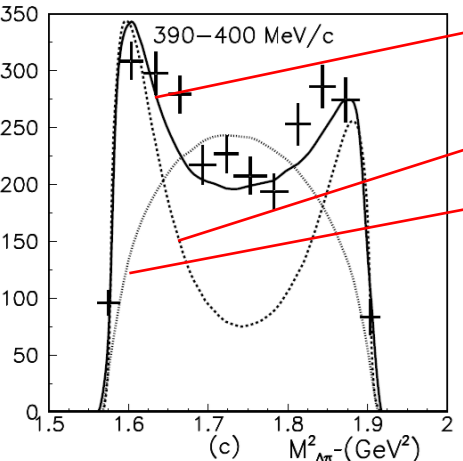
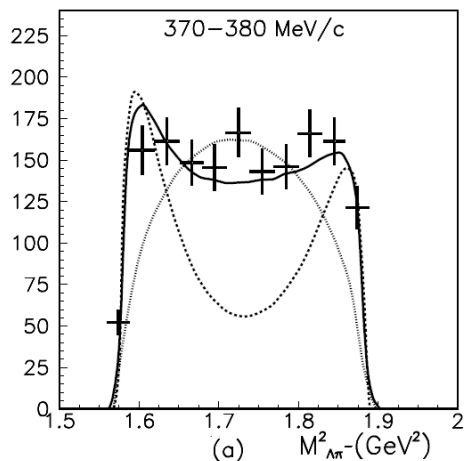
J. J. Wu, S. Dulat and B. S. Zou PRC 81, 045210



$K^- p \rightarrow \Lambda \pi^+ \pi^-$

$P_K = 0.3\text{-}0.6 \text{ GeV}$

J. J. Wu, S. Dulat and B. S. Zou PRC 81,045210

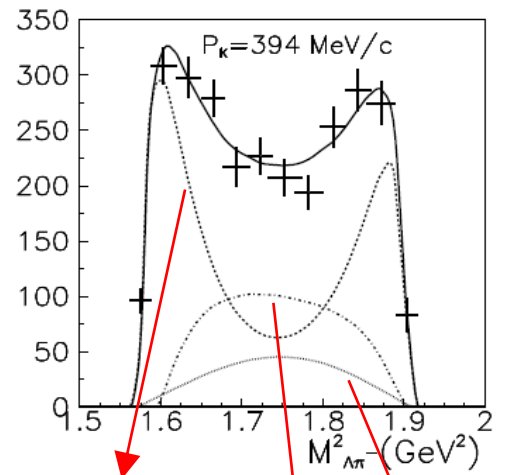
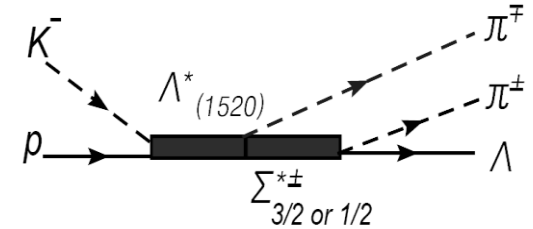


59% $\Sigma^*(3/2^+)$ + 41% $\Sigma^*(1/2^-)$

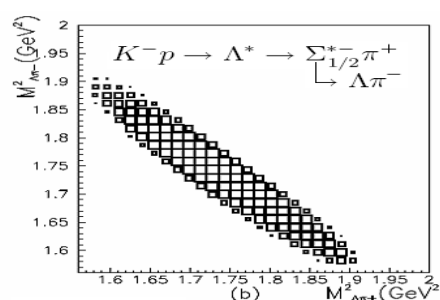
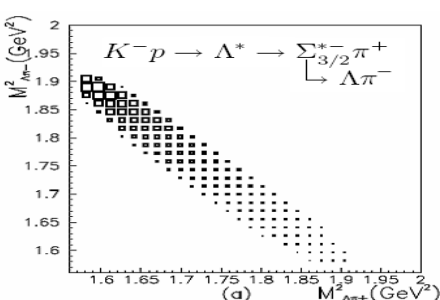
100% $\Sigma^*(3/2^+)$

Phase space

First reason: S-wave between the $\Sigma^*(3/2^+)$ and π^+ ; but P-wave between the $\Sigma^*(1/2^-)$ and π^+ .



59% $\Sigma^*(3/2^+)$
Interference
12.5% $\Sigma^*(1/2^-)$



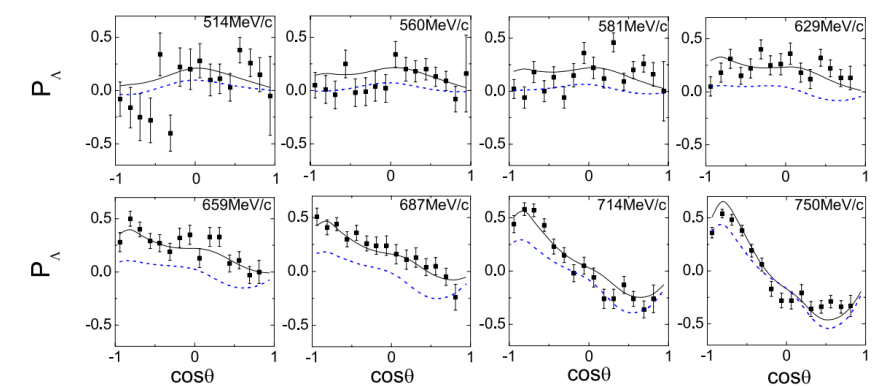
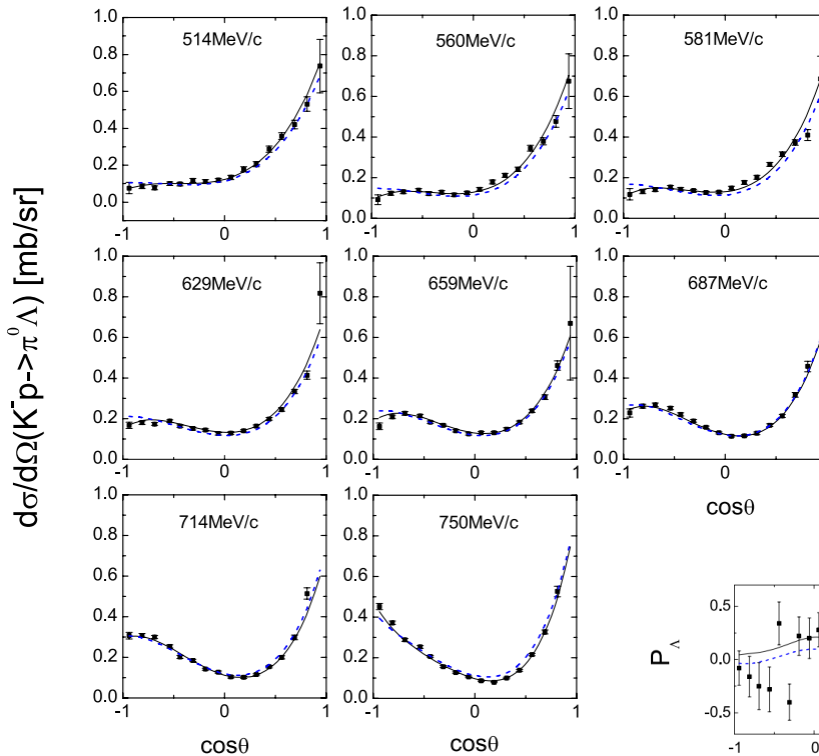
Second reason: the width of $\Sigma^*(3/2^+)$ is 35.5 MeV; but that of $\Sigma^*(1/2^-)$ is 118.6 MeV from fit before.



$$K^- p \rightarrow \pi^0 \Lambda$$

The research for the possible new $\Sigma(\frac{1}{2}^-)$ near 1380 MeV has always been our concern, and previous work has shown some evidence of it [13–15]. In this work, we also check whether this data set is compatible with the existence of the $\Sigma(1380)$. Without including the $\Sigma(1635)$, we try to include a $\Sigma(\frac{1}{2}^-)$, and constrain its mass above 1360 MeV. From our analysis, the best fit gives $\chi^2 = 385$ a minimum mass, a small coupling constant $g_{KN\Sigma(\frac{1}{2}^-)} g_{\Sigma(\frac{1}{2}^-)\pi\Lambda} \sim -1.26$ and width around 315 MeV. This shows that the existence of a $\Sigma(\frac{1}{2}^-)$ near 1380 MeV with sizeable couplings is not ruled out by the present data, although there is no strong evidence of it. This result is understandable since 1380 MeV is much smaller than the energy range of the experiment.

P. Gao B.S. Zou *Nucl.Phys.A* 867 (2011) 41-51



$\Sigma(1189), \Sigma(1385),$
 $\Sigma(1670), \Sigma(1775),$

$$\chi^2 = 763/248$$

$\Sigma(1635)(1/2^+)$

$$\chi^2 = 223/248$$

Crystal Ball Collaboration
PRC 80, 025204 (2009).

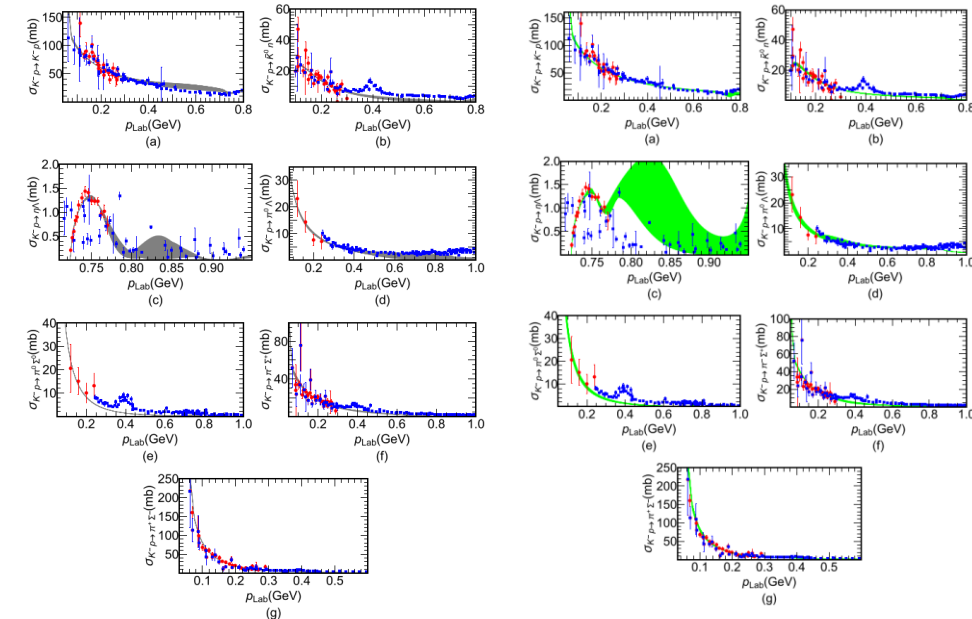
Situation is similar when consider $K^- n \rightarrow \pi \Lambda$

P. Gao J. Shi and B.S. Zou *PRC* 86 (2012) 025201



$$K^- p \rightarrow K^- p, \bar{K}^0 n, \eta\Lambda, \pi^0\Lambda, \pi^0\Sigma^0, \pi^\mp\Sigma^\pm\bar{\Sigma}^\mp$$

K. P. Khemchandani, A. Martínez Torres and J. A. Oller, PRD 100 (2019) 015208



Fit I

Fit III

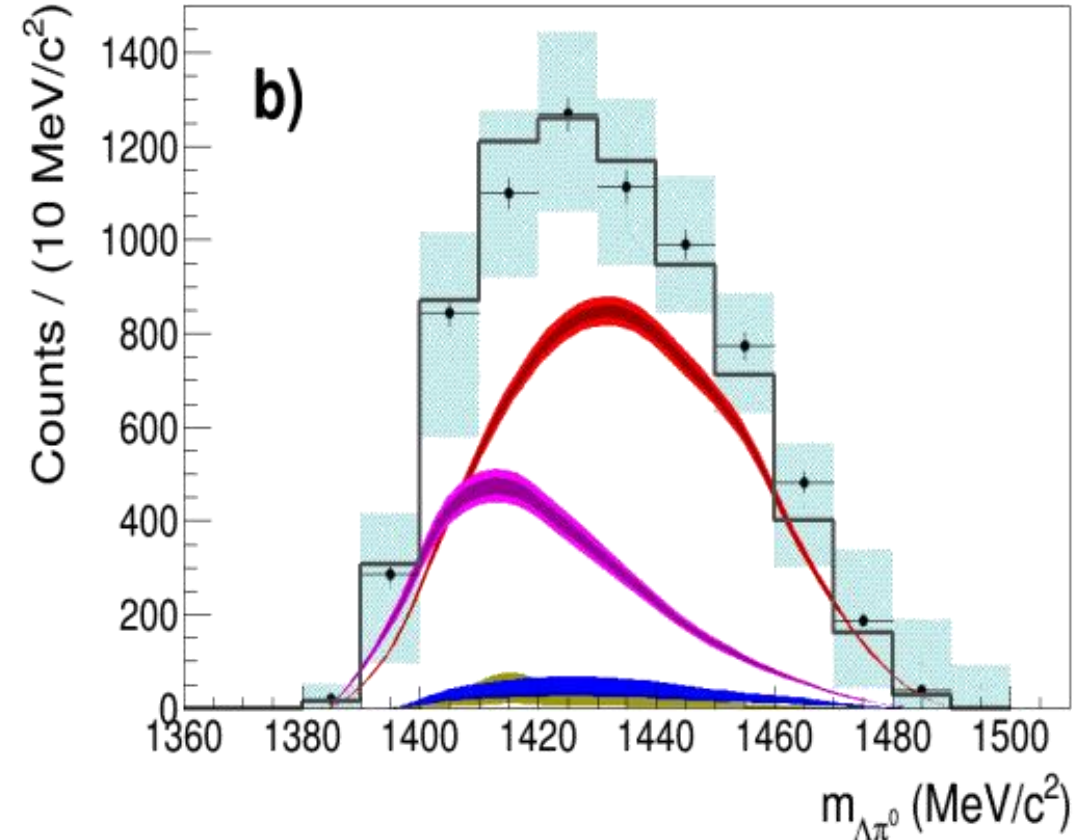
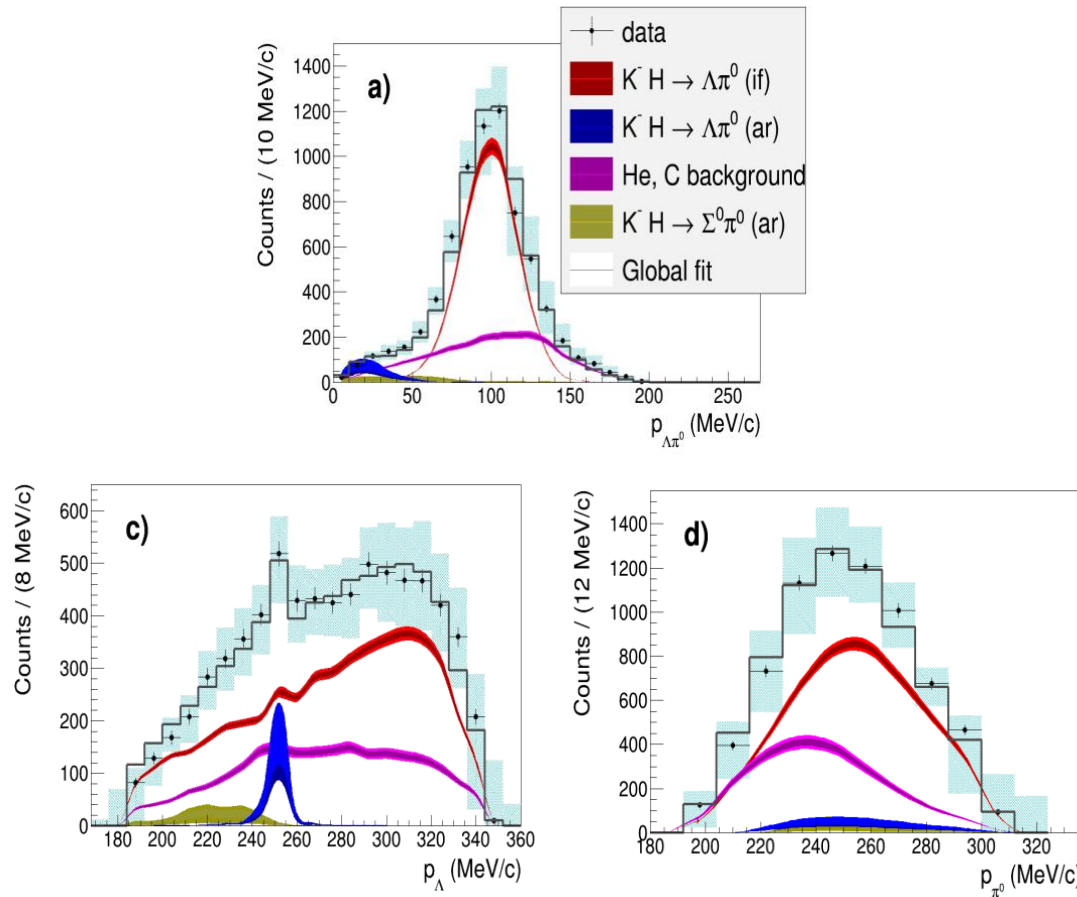


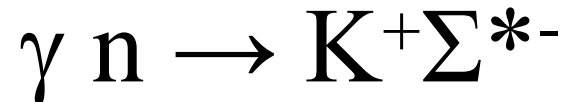
TABLE IV. Pole positions and couplings of the $I(J^P) = 1(1/2^-)$ states found in our work. The central values and errors were obtained as explained in the caption of Table I (for the sake of space, the errors are represented as superscripts).

	Σ 's around 1400 MeV		$\Sigma(1620)$ or $\Sigma(1670)$	$\Sigma(1900)$
Fit I	$1396^{+1} - i 5^{+2}$	$1367^{+24} - i 57^{+21}$	$1630^{+33} - i 104^{+13}$	$1853^{+10} - i 150^{+10}$
Fit II	—	$1399^{+35} - i 36^{+9}$	—	—
$\bar{K}N$	$0.18^{+0.03} + i 0.14^{+0.05}$ —	$0.08^{+0.48} + i 0.52^{+0.73}$ $0.50^{+0.29} + i 0.33^{+0.18}$	$1.47^{+0.08} - i 0.017^{+0.07}$ —	$-0.86^{+0.03} + i 0.79^{+0.02}$ —
$K\Sigma$	$1.06^{+0.22} + i 1.45^{+0.12}$ —	$0.62^{+0.47} - i 0.42^{+1.00}$ $0.81^{+0.42} + i 0.41^{+0.15}$	$2.89^{+0.26} - i 0.65^{+0.24}$ —	$0.84^{+0.03} - i 0.39^{+0.05}$ —
$\pi\Sigma$	$-0.17^{+0.09} - i 0.020^{+0.03}$ —	$0.77^{+0.96} - i 0.67^{+1.22}$ $1.08^{+0.12} + i 0.19^{+0.21}$	$0.71^{+0.33} - i 1.63^{+0.19}$ —	$-0.02^{+0.04} + i 0.32^{+0.08}$ —
$\pi\Lambda$	$0.03^{+0.10} + i 0.07^{+0.06}$ —	$-0.91^{+1.32} + i 0.39^{+0.81}$ $-1.40^{+0.18} - i 0.07^{+0.10}$	$-0.26^{+0.34} - i 0.23^{+0.18}$ —	$0.36^{+0.2} + i 1.54^{+0.04}$ —
$\eta\Sigma$	$-0.43^{+0.03} - i 0.23^{+0.09}$ —	$0.31^{+0.31} - i 0.59^{+1.12}$ $0.27^{+0.10} - i 0.19^{+0.11}$	$-2.14^{+0.24} - i 0.13^{+0.11}$ —	$0.07^{+0.03} - i 0.43^{+0.02}$ —
\bar{K}^*N	$0.04^{+0.10} + i 0.15^{+0.07}$ —	$-1.69^{+1.99} + i 0.31^{+0.68}$ $-3.46^{+0.21} - i 0.06^{+0.15}$	$-0.31^{+0.09} - i 0.11^{+0.16}$ —	$0.71^{+0.05} - i 0.05^{+0.02}$ —
$K^*\Sigma$	$-0.50^{+0.22} - i 0.38^{+0.08}$ —	$1.40^{+2.11} - i 1.10^{+2.38}$ $-0.01^{+0.59} - i 0.21^{+0.08}$	$-1.80^{+0.47} - i 0.37^{+0.14}$ —	$-0.98^{+0.14} - i 0.72^{+0.06}$ —
$\rho\Sigma$	$-0.15^{+0.07} - i 0.14^{+0.04}$ —	$0.76^{+1.02} - i 0.58^{+0.85}$ $3.60^{+0.61} - i 0.69^{+0.16}$	$-0.76^{+0.18} - i 0.53^{+0.49}$ —	$-1.10^{+0.04} - i 0.34^{+0.03}$ —
$\rho\Lambda$	$0.36^{+0.18} + i 0.29^{+0.07}$ —	$-0.95^{+1.50} + i 0.93^{+1.84}$ $-1.26^{+0.19} + i 0.09^{+0.07}$	$2.44^{+0.50} + i 0.94^{+0.27}$ —	$1.51^{+0.25} + i 0.82^{+0.09}$ —
$\omega\Sigma$	$-0.15^{+0.11} - i 0.14^{+0.05}$ —	$1.03^{+1.35} - i 0.55^{+1.10}$ $2.15^{+0.20} - i 0.13^{+0.09}$	$-0.14^{+0.23} - i 0.44^{+0.14}$ —	$-0.64^{+0.10} - i 0.23^{+0.04}$ —
$\phi\Sigma$	$0.27^{+0.17} + i 0.24^{+0.08}$ —	$-1.73^{+2.27} + i 0.90^{+1.82}$ $-3.23^{+0.39} + i 0.20^{+0.11}$	$0.42^{+0.38} + i 0.53^{+0.24}$ —	$1.04^{+0.20} + i 0.39^{+0.07}$ —

$$K^- p \rightarrow (\Sigma^0/\Lambda) \pi^0$$

AMADEUS collaboration arXiv:2210.10342 based on the data of 2004/2005 KLOE



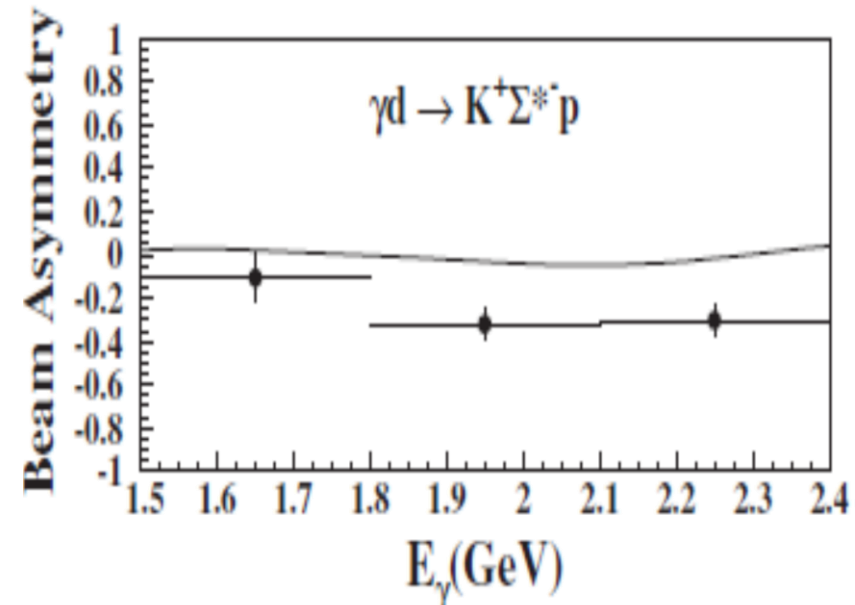


- Total cross section $\gamma n \rightarrow K^+ \Sigma^{*-}$ of CLAS well described.
- differential cross section $\gamma n \rightarrow K^+ \Sigma^{*-}$ of LEPS data also be described, but not for the beam asymmetry A_{beam} .

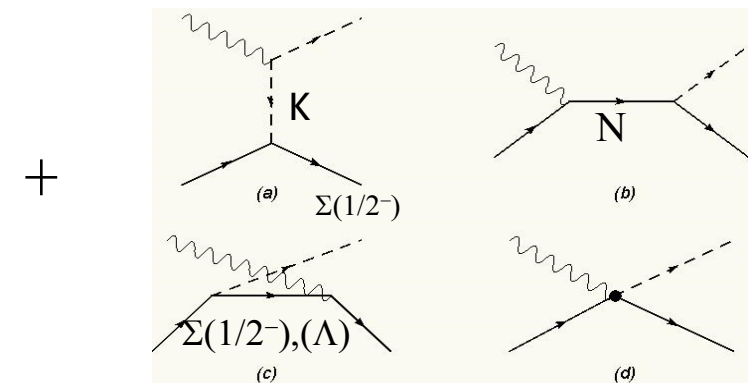
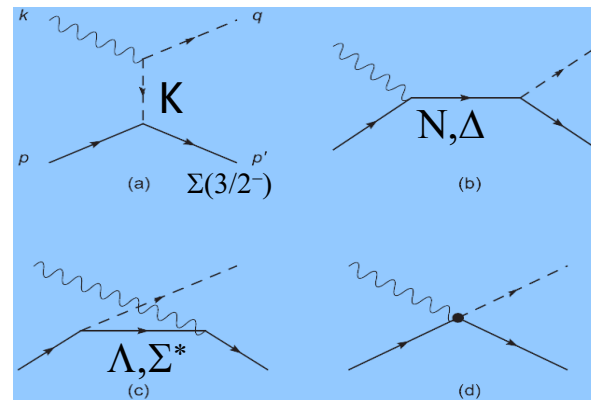
$$A_{beam} = \frac{\sigma_{\perp} - \sigma_{\parallel}}{\sigma_{\perp} + \sigma_{\parallel}}$$

σ_{\perp} and σ_{\parallel} denote the cross sections for beam polarization vertical and parallel to reaction plane, respectively.

a. Including $\Sigma(1380)1/2^-$ Puze Gao, J. J. Wu, B. S. Zou, PRC81:055203



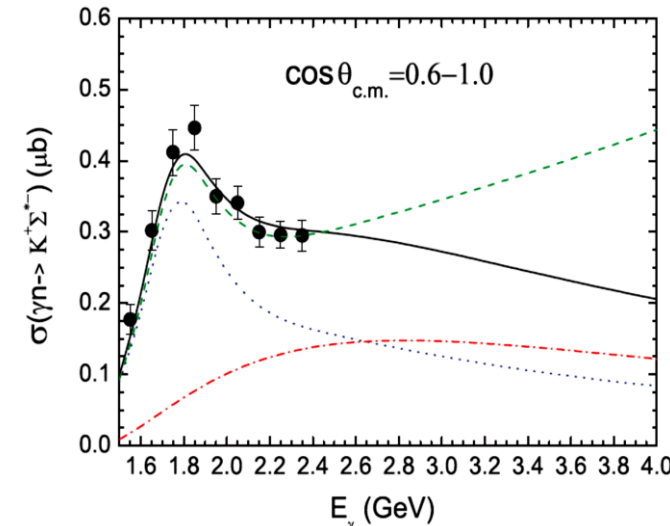
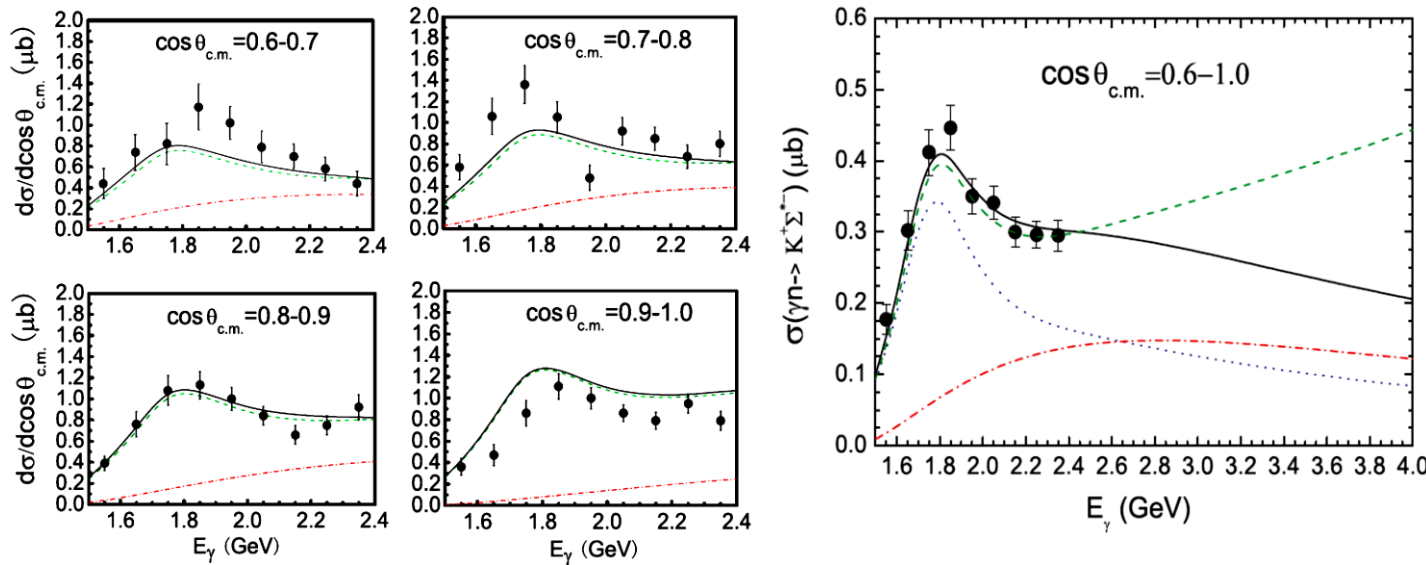
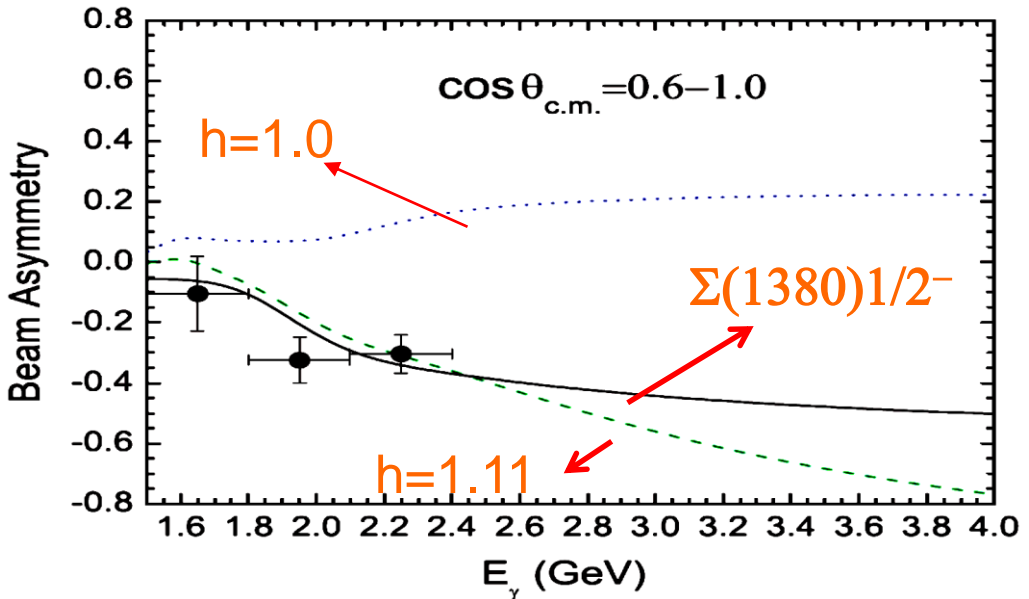
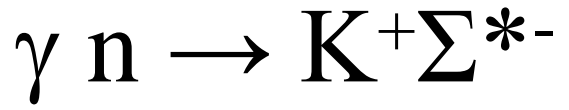
Hicks, et.al. (LEPS), PRL102,012501(2009)



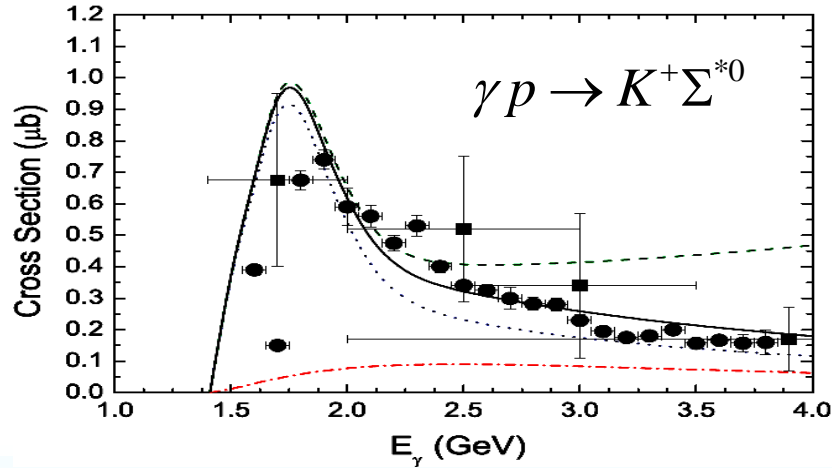
b. Change h in contact term

- **h=1** for $\gamma \pi \rightarrow K^+ \Sigma^{*0}$ to describe the total cross section.
- **Free h=1.11** for $\vec{\gamma} n \rightarrow K^+ \Sigma^-$ without $\Sigma(1380)1/2^-$.





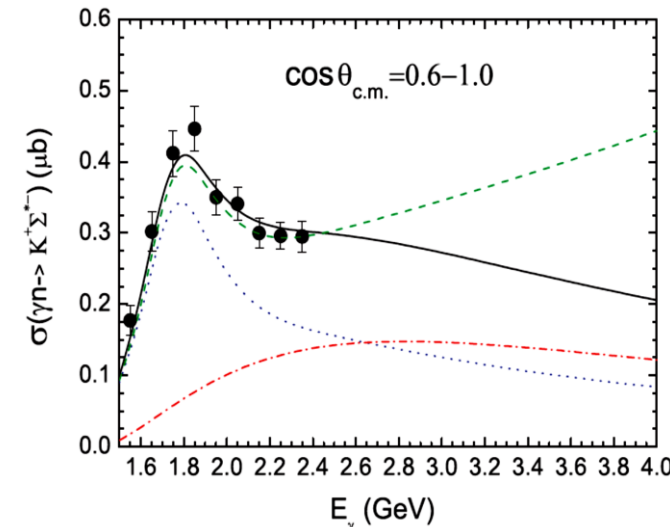
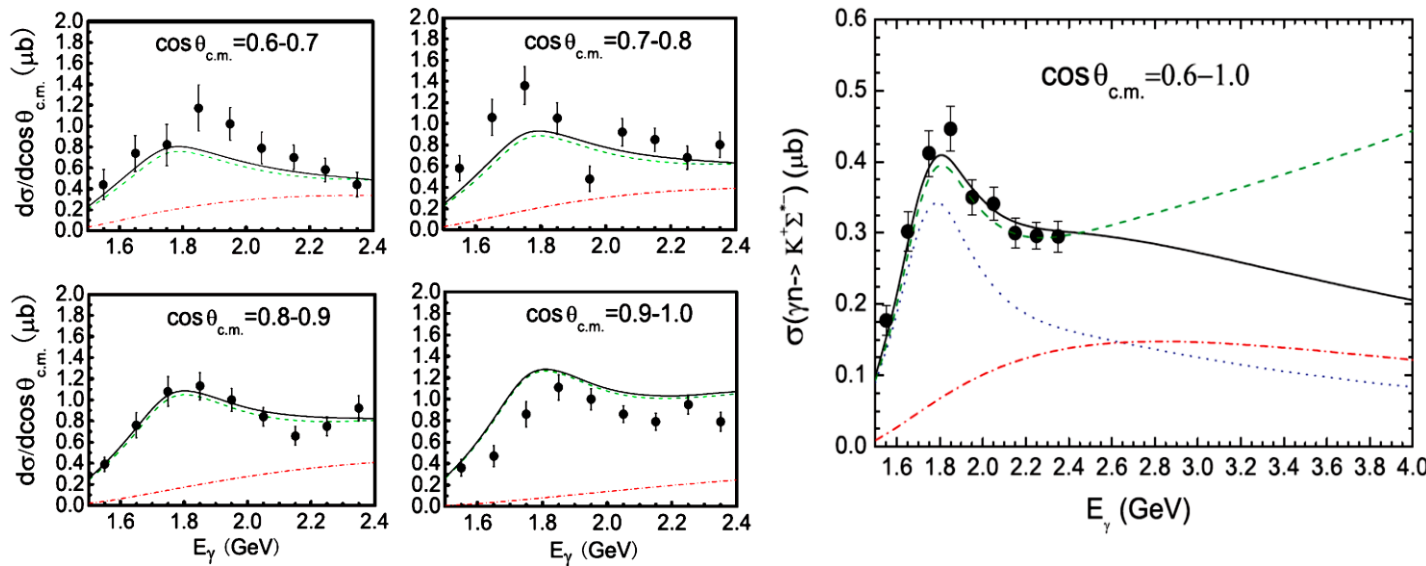
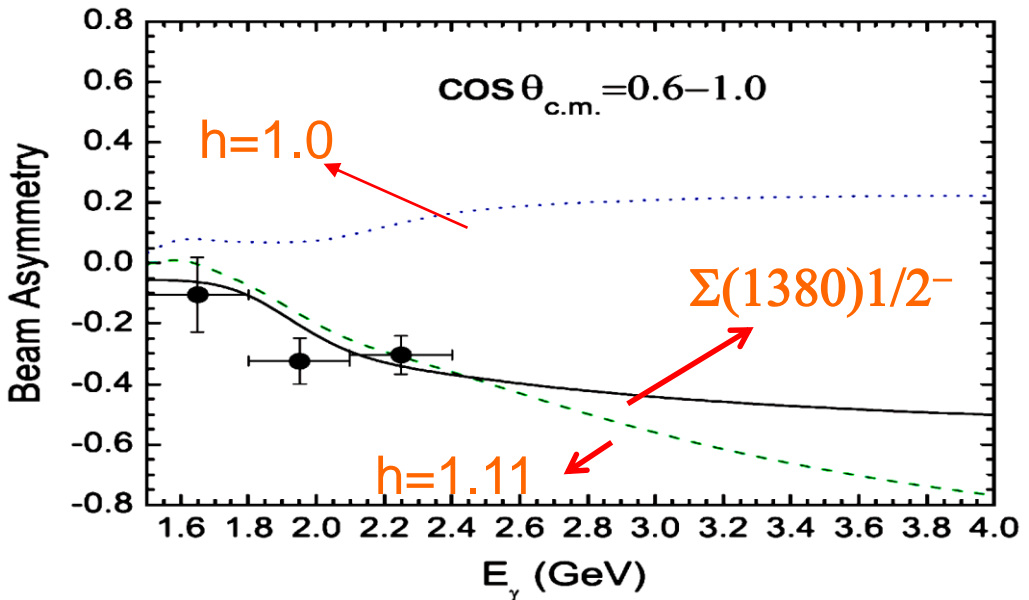
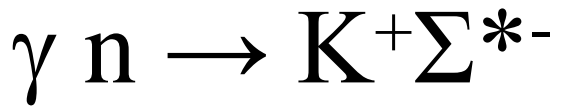
$d\sigma/d\cos\theta_{\text{c.m.}}$ for $\gamma n \rightarrow K\Sigma^*$ compared with LEPS data



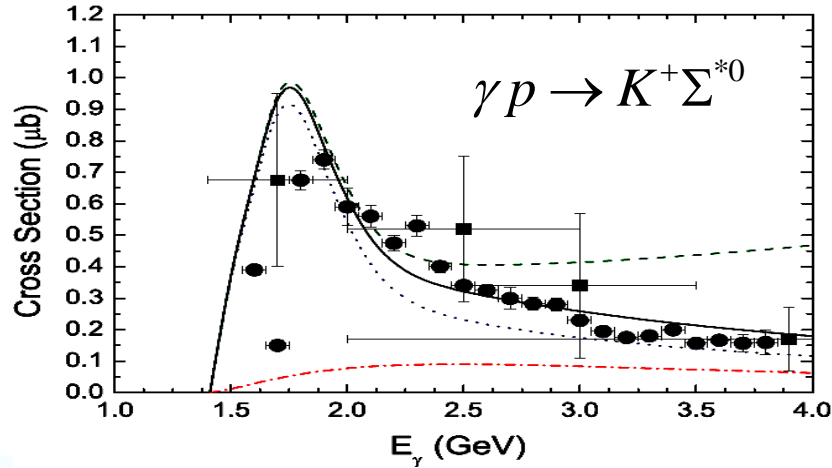
Puze Gao, J. J. Wu, B. S. Zou, PRC81:055203



中国科学院大学
University of Chinese Academy of Sciences



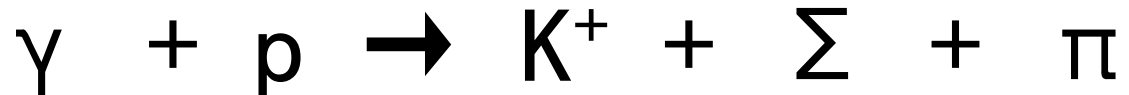
$d\sigma/d\cos\theta_{\text{c.m.}}$ for $\gamma n \rightarrow K\Sigma^*$ compared with LEPS data



Puze Gao, J. J. Wu, B. S. Zou, PRC81:055203



中国科学院大学
University of Chinese Academy of Sciences



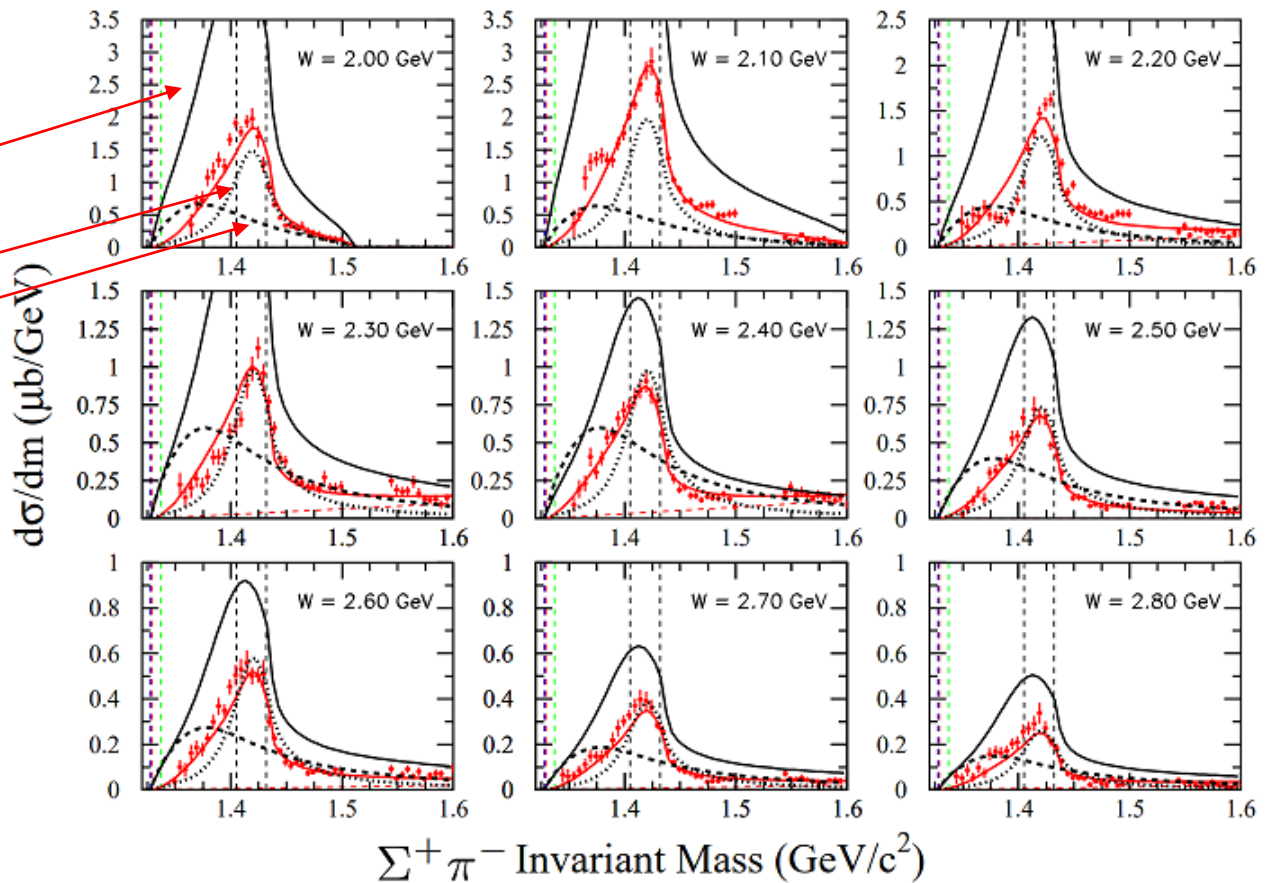
CLAS Phys.Rev.C 87 (2013) 3, 035206

TABLE III. Results of the fit using one $I = 0$ and two $I = 1$ Breit-Wigner line shapes.

Amplitude	Centroid m_R (MeV/c ²)	Width $\Gamma_{I,1}^0$ (MeV/c ²)	Phase $\Delta\Phi_I$ (radians)	Flatté Factor
$I = 0$	1338 ± 10	85 ± 10	N/A	0.91 ± 0.20
$I = 1$ (narrow)	1413 ± 10	52 ± 10	2.0 ± 0.2	0.41 ± 0.20
$I = 1$ (broad)	1394 ± 20	149 ± 40	0.1 ± 0.3	N/A

amplitude was added to include the $\Sigma^+\pi^-$ and $\Sigma^-\pi^+$ final state combinations. However, it was found that a much better fit could be obtained with a *single* $I = 0$ amplitude and two separate coherent $I = 1$ amplitudes. This is the result we show here. More complete details of the fits will be given in the separate paper [47], but here we present the “best fit” results.

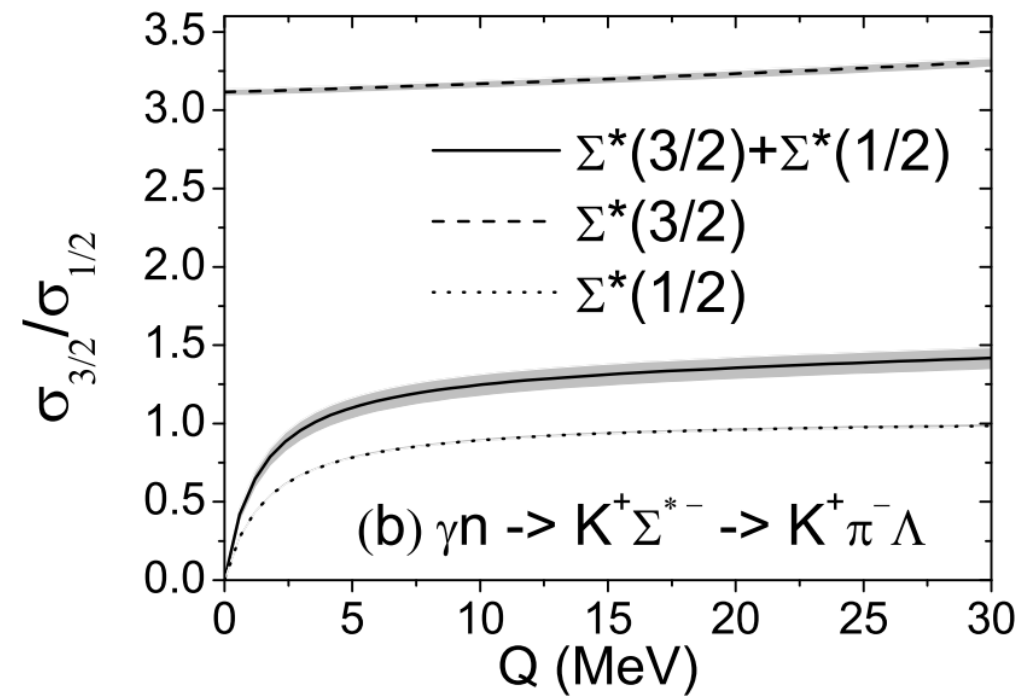
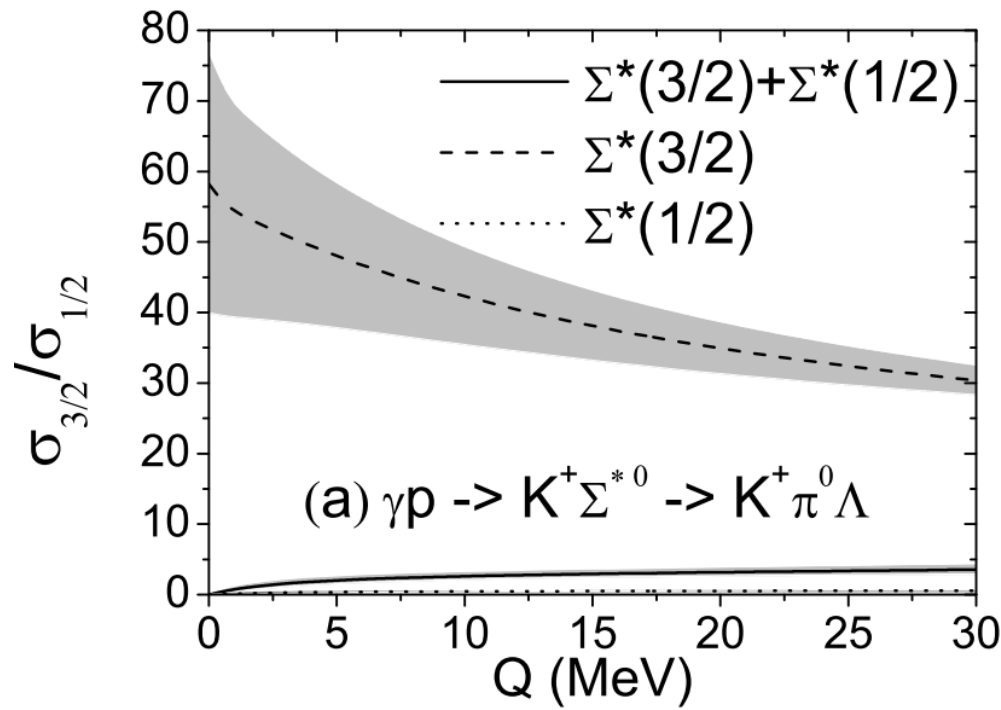
The fits were made to a reduced data set in order to





Y. H. Chen and B.S. Zou *Phys.Rev.C 88 (2013) , 024304*

The helicity cross sections $\sigma_{3/2}$ and $\sigma_{1/2}$, which correspond to spin-parallel and spin-antiparallel states of the photon and nucleon respectively.





L. Roca and E. Oset *Phys.Rev.C* 88 (2013) 3, 055206

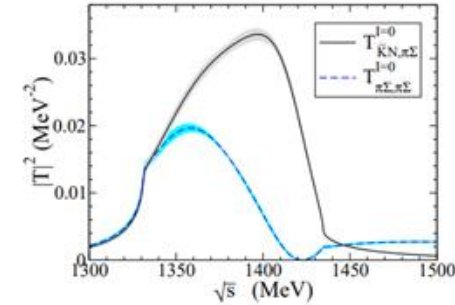
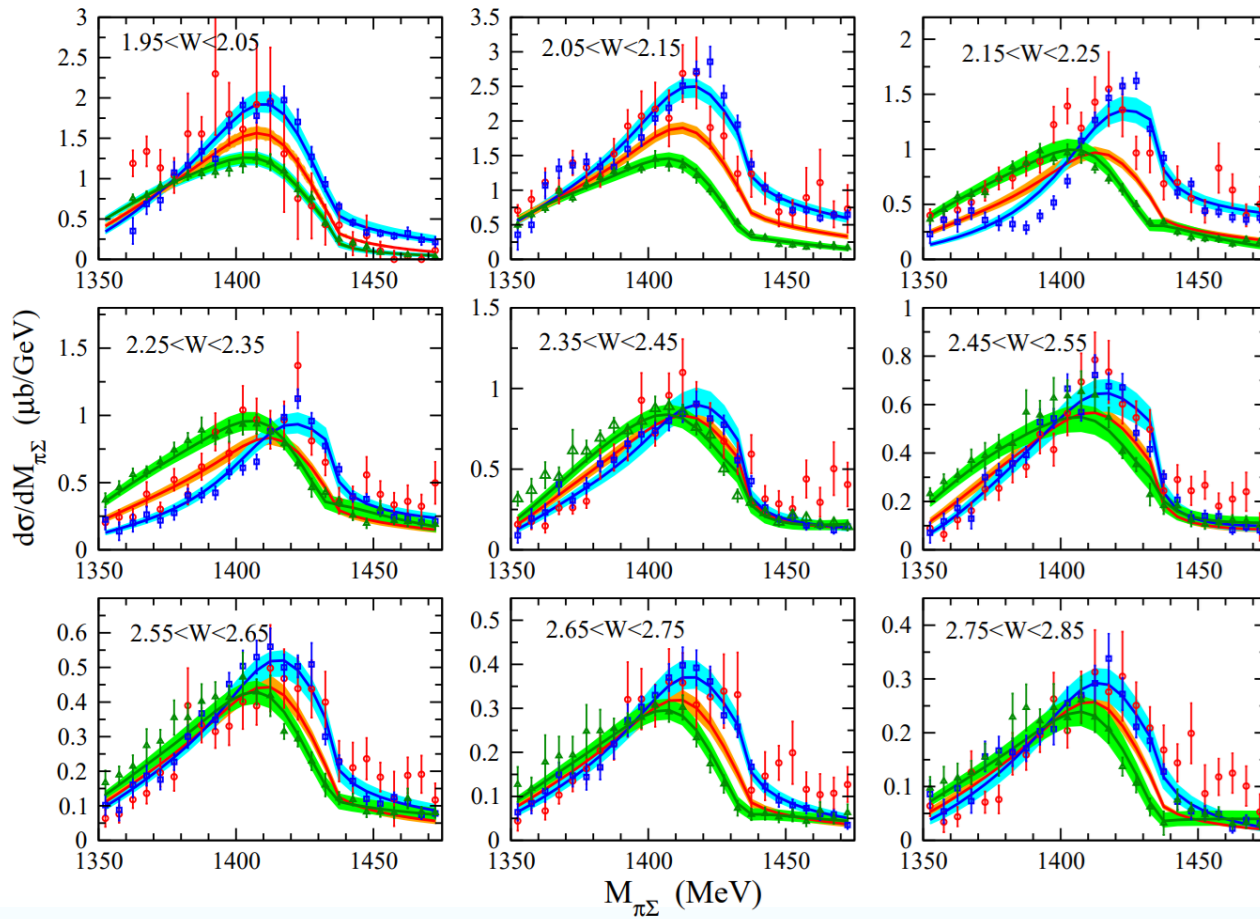


FIG. 6. (Color online) Modulus squared of the $I = 0$ meson-baryon unitarized amplitudes $T_{\pi\Sigma, \pi\Sigma}^{I=0}$ (solid line), $T_{\bar{K}N, \pi\Sigma}^{I=0}$ (dashed line) and $T_{\pi\Lambda, \pi\Sigma}^{I=0}$ (dash-dotted line).

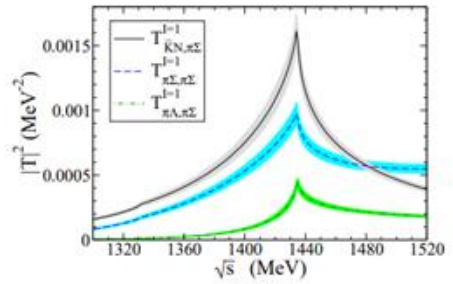


FIG. 7. (Color online) Modulus squared of the $I = 1$ meson-baryon unitarized amplitudes $T_{\pi\Sigma, \pi\Sigma}^{I=1}$ (solid line), $T_{\bar{K}N, \pi\Sigma}^{I=1}$ (dashed line) and $T_{\pi\Lambda, \pi\Sigma}^{I=1}$ (dash-dotted line).

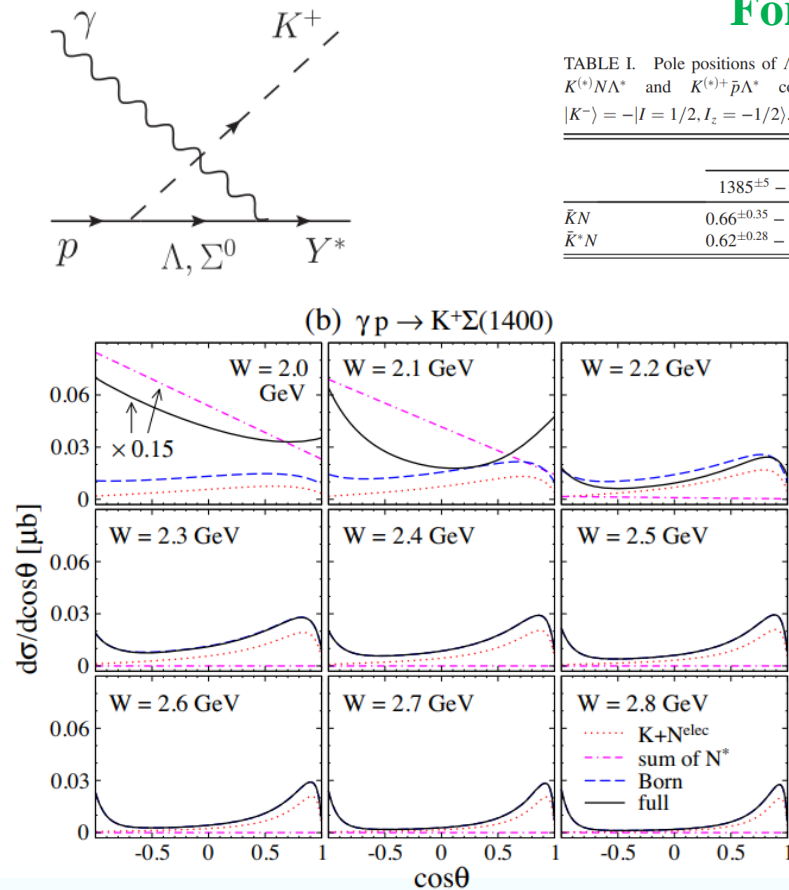
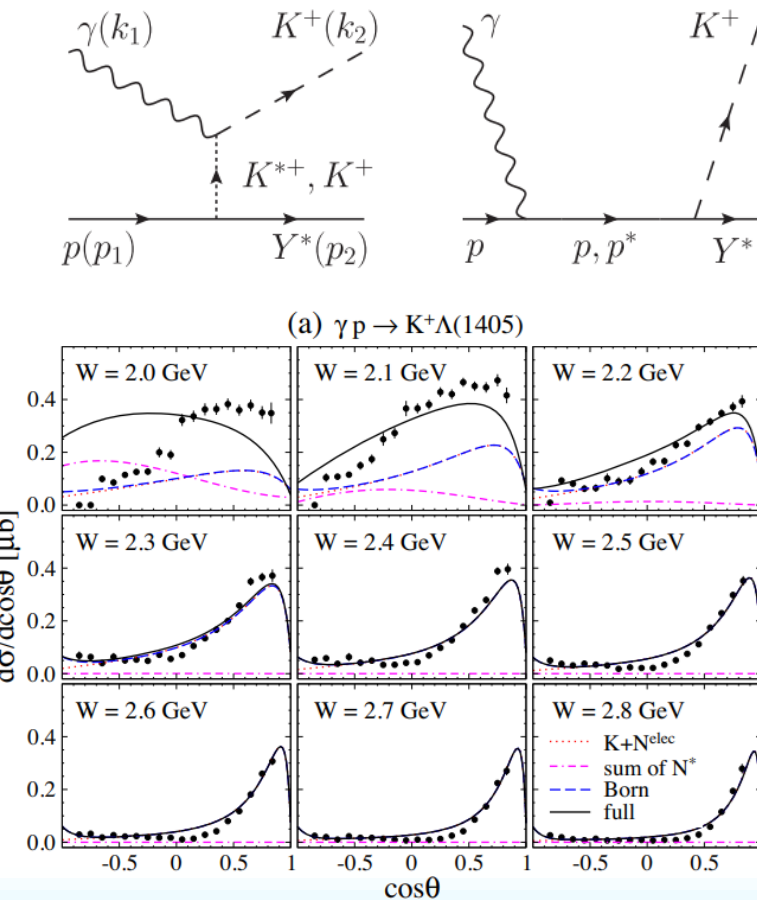
Two poles for $\Lambda(1405)$

pole but then decrease above threshold with a non resonant shape. This means that, for the $I = 1$ amplitudes considered here, even if there is not an explicit pole in the usual unphysical Riemann sheet, an accumulation of strength is present on the real axis in the physical sheet, under the appearance of a cusp. In Figs. 6 and 7 we show the $I = 0$ and $I = 1$ meson-baryon amplitudes with the

	$I = 0$	$I = 1$
poles	1352 – 48 <i>i</i>	1419 – 29 <i>i</i>
$ g_{\bar{K}N} $	2.71	3.06
$ g_{\pi\Sigma} $	2.96	1.96

$\gamma N \rightarrow K^+ \Sigma^*$

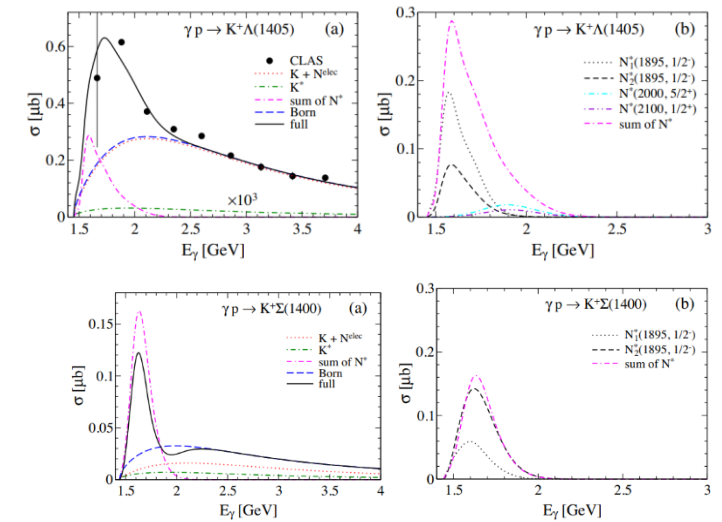
S.-h. Kim, K. P. Khemchandani, A. Martinez Torres, S. Nam, A. Hosaka *Phys.Rev.D* 103 (2021) , 114017



For $K\bar{p}$ *PRD* 100 (2019) 015208

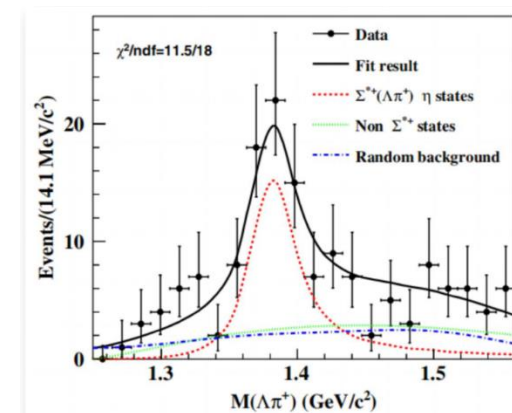
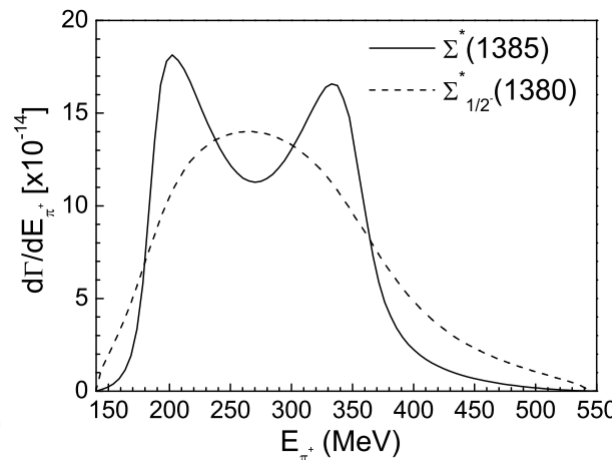
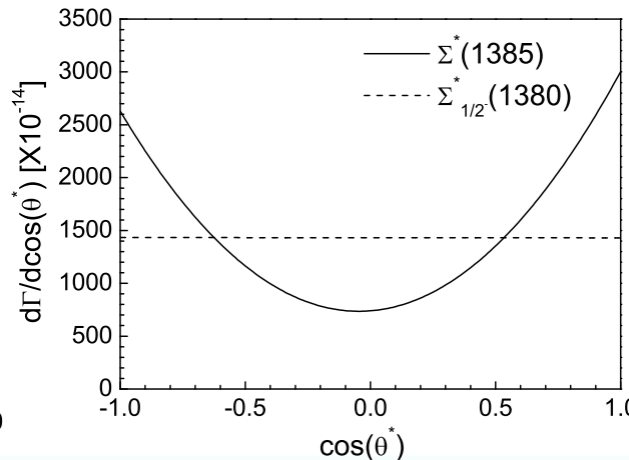
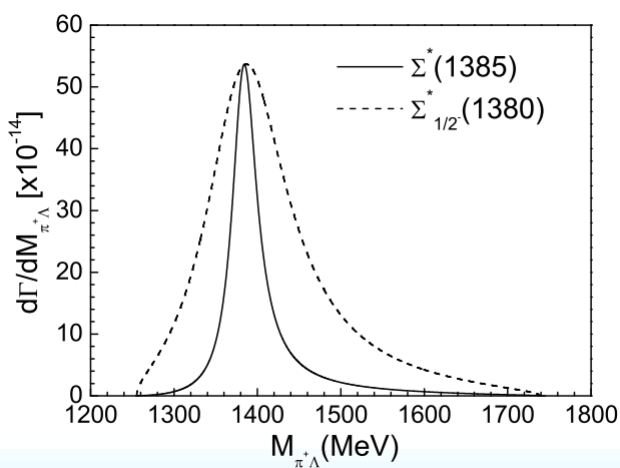
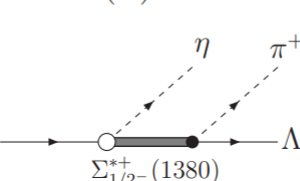
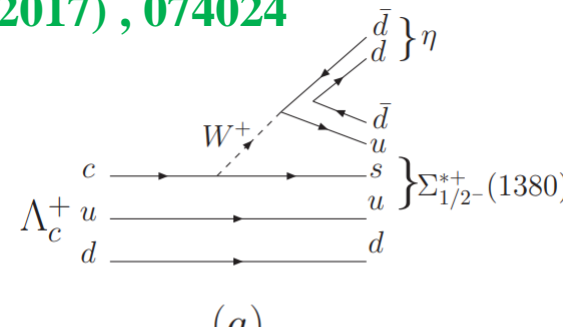
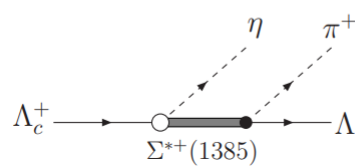
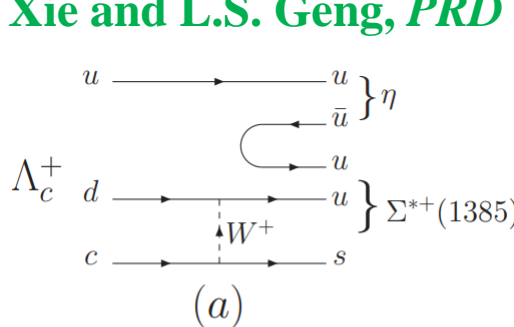
TABLE I. Pole positions of $\Lambda(1405)$ and $\Sigma(1400)$ and their couplings to $\bar{K}N$ and \bar{K}^*N (in the isospin base) [21]. Note that the $K^{(*)}N\Lambda^*$ and $K^{(*)}\bar{p}\Lambda^*$ couplings are related by the Clebsch-Gordan coefficient $\frac{1}{\sqrt{2}}$, following the convention $|K^- \rangle = -|I = 1/2, I_z = -1/2\rangle$. Also the $K^{(*)}N\Sigma^*$ and $K^{(*)}\bar{p}\Sigma^0$ couplings are related by a factor $-\frac{1}{\sqrt{2}}$.

	$\Lambda(1405)$	Σ 's around 1400 MeV
$\bar{K}N$	$1385^{\pm 5} - i124^{\pm 10}$	$1426^{\pm 1} - i15^{\pm 2}$
\bar{K}^*N	$0.66^{\pm 0.35} - i1.93^{\pm 0.12}$	$2.43^{\pm 0.16} + i0.63^{\pm 0.23}$

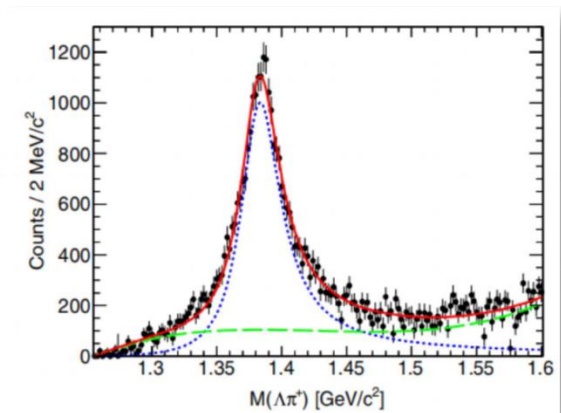


$\Lambda_c^+ \rightarrow \eta\pi^+\Lambda$

J.J. Xie and L.S. Geng, PRD 95 (2017) , 074024



BESIII, PRD99, 032010
(2019)



Belle,
PRD103(2021)052005

No clear signal

G.Y. Wang, N.-C. Wei, H.M Yang, E. Wang, L.-S. Geng
PRD 106 (2022) 5, 056001



中国科学院大学
University of Chinese Academy of Sciences

$$\Lambda_C^+ \rightarrow \pi^+ \pi^- \pi^+ \Lambda$$

Belle, *PRL* 130 (2023) , 151903

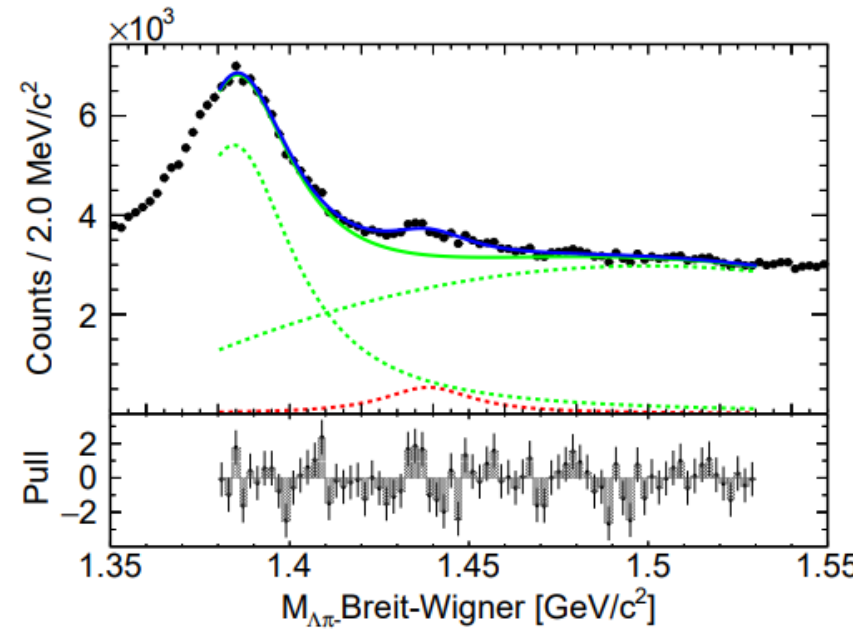
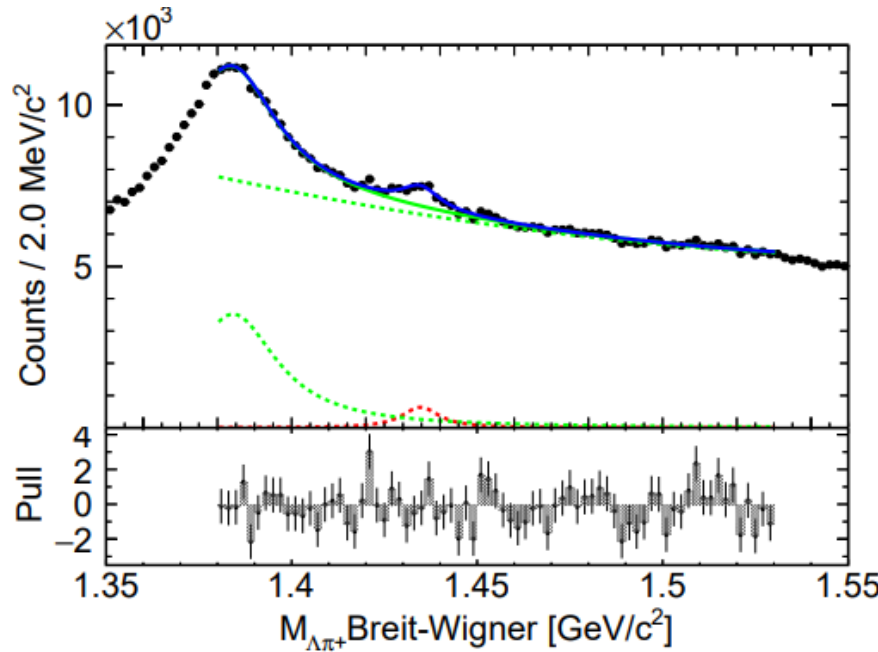


TABLE I. Breit-Wigner fitting results. The quoted errors are statistical only.

Mode	E_{BW} [MeV/ c^2]	Γ [MeV/ c^2]	χ^2 / NDF
$\Lambda\pi^+$	1434.3 ± 0.6	11.5 ± 2.8	74.4/68
$\Lambda\pi^-$	1438.5 ± 0.9	33.0 ± 7.5	92.3/68



$\Lambda p \rightarrow \Lambda p \pi^0$

J.J. Xie, J.J. Wu and B.S. Zou *Phys.Rev.C* 90 (2014) , 055204

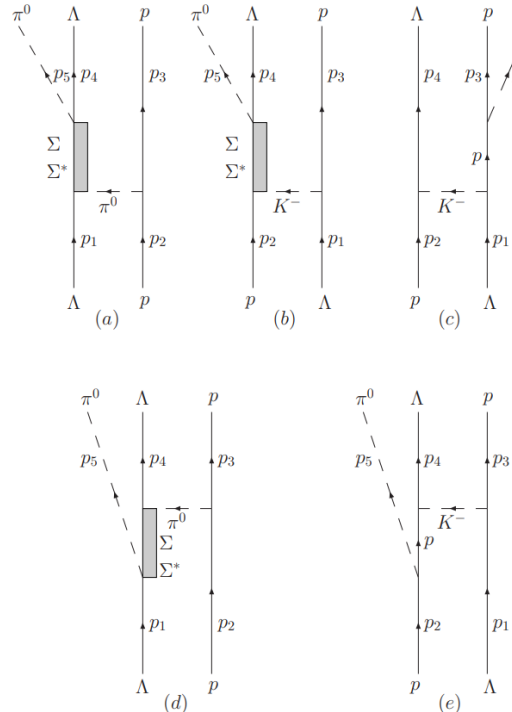
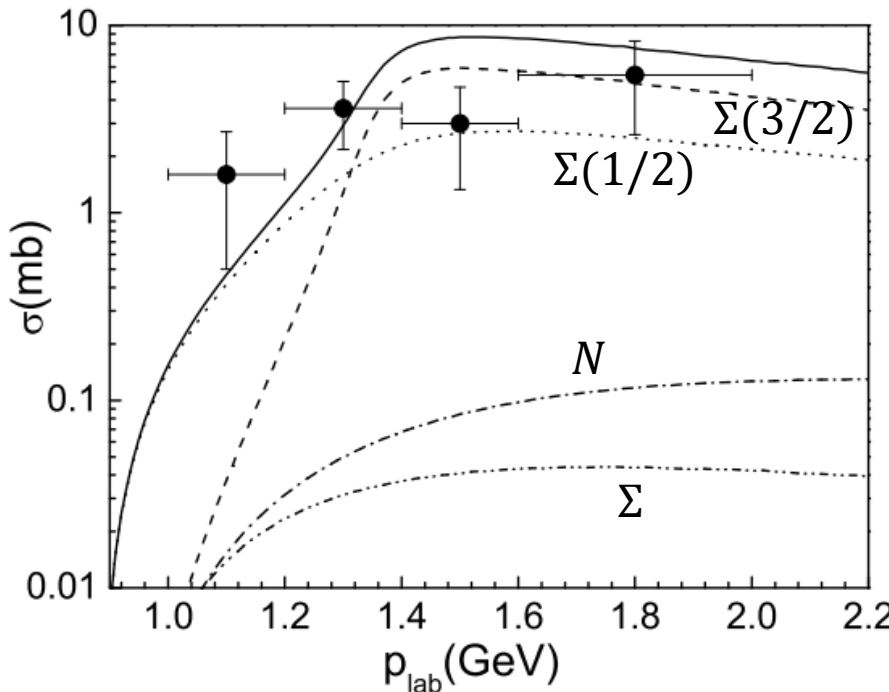
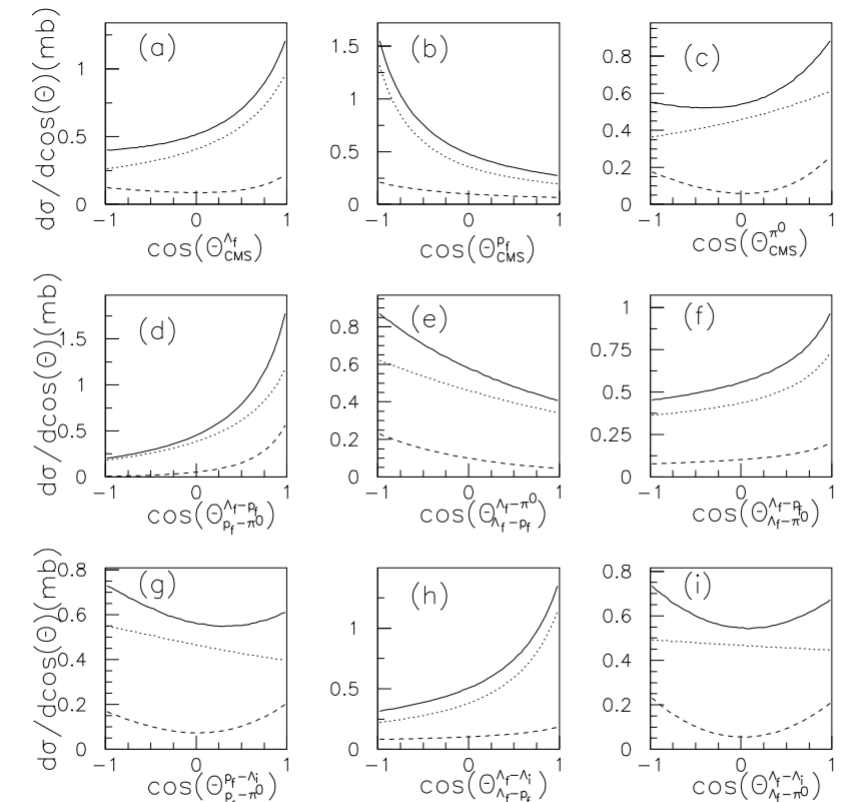


FIG. 1: Feynman diagrams for $\Lambda p \rightarrow \Lambda p\pi^0$ reaction.

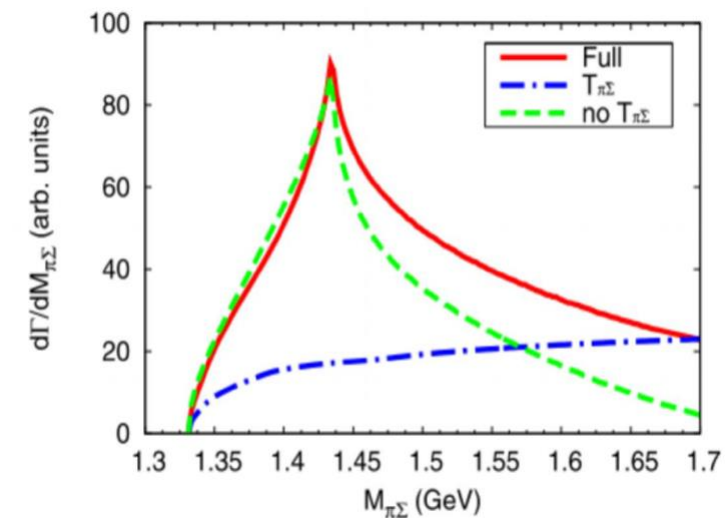
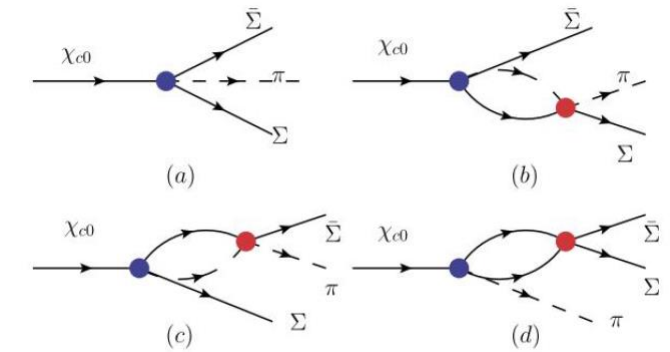
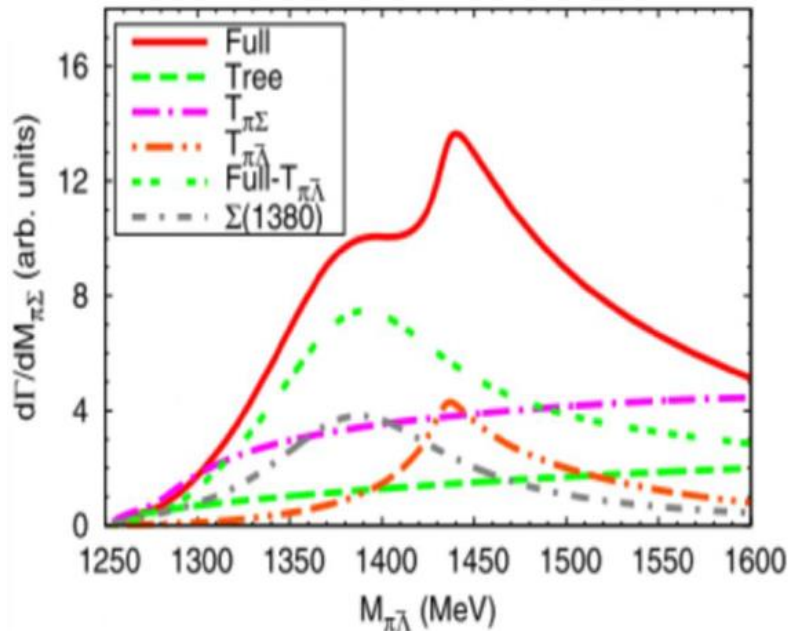
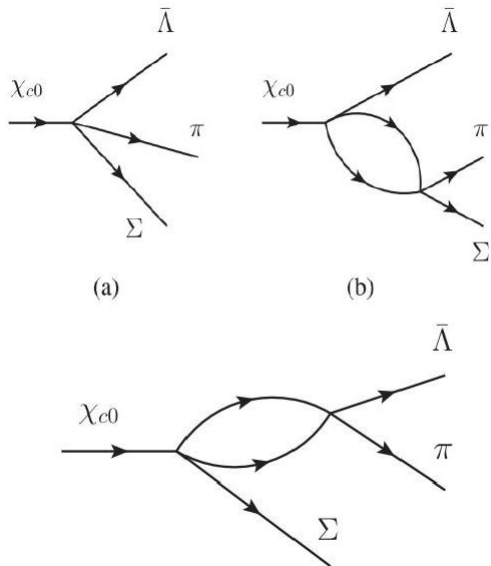


Angular differential cross sections for the $\Lambda p \rightarrow \Lambda p\pi^0$ reaction in CMS [(a): $\Theta_{\Lambda f}^{\Lambda f}$, (b): $\Theta_{\Lambda f}^{p_f}$, (c): $\Theta_{\Lambda f}^{\pi^0}$], helicity [(d): $\Theta_{p_f-\pi^0}^{\Lambda f}$, (e): $\Theta_{\Lambda f-p_f}^{\Lambda f-\pi^0}$, (f): $\Theta_{\Lambda f-p_f}^{\Lambda f-p_f}$], and Gottfried-Jackson [(g): $\Theta_{p_f-\pi^0}^{p_f-\Lambda_i}$, (h): $\Theta_{\Lambda f-p_f}^{\Lambda f-\Lambda_i}$, (i): $\Theta_{\Lambda f-\pi^0}^{\Lambda f-\Lambda_i}$] reference frames. The dashed and solid curves stand the contributions of the $\Sigma^*(1385)$ and $\Sigma^*(1380)$, respectively. The results are obtained at $p_{\text{lab}} = 1.2$ GeV.



$$\chi_{c0} \rightarrow \bar{\Sigma}\Sigma\pi, \bar{\Lambda}\Sigma\pi$$

E. Wnng , J.J. Xie, and E. Oset, PLB753 (2016) 526, PRD98 (2018)114017



$$\bar{\nu}_l p \rightarrow l^+ \phi B$$

X.L. Ren, E. Oset, L. Alvarez-Ruso, and M.J. Vicente Vacas, PRC 91 (2015) , 045201

We have studied the strangeness changing antineutrino induced reactions $\bar{\nu}_l p \rightarrow l^+ \phi B$, with $\phi B = K^- p$, $\bar{K}^0 n$, $\pi^0 \Lambda$, $\pi^0 \Sigma^0$, $\eta \Lambda$, $\eta \Sigma^0$, $\pi^+ \Sigma^-$, $\pi^- \Sigma^+$, $K^+ \Xi^-$ and $K^0 \Xi^0$, using a chiral unitary approach. These ten coupled channels are allowed to interact strongly, using a kernel derived from the chiral Lagrangians. This interaction generates two $\Lambda(1405)$ poles, leading to a clear single peak in the $\pi\Sigma$ invariant mass distributions. At backward scattering angles in the center of mass frame, $\bar{\nu}_\mu p \rightarrow \mu^+ \pi^0 \Sigma^0$ is dominated by the $\Lambda(1405)$ state at around 1420 MeV while the lighter state becomes relevant as the angle decreases, leading to an asymmetric line shape. In addition, there are substantial differences in the shape of $\pi\Sigma$ invariant mass distributions for the three charge channels. If observed, these differences would provide valuable information on a claimed isospin $I = 1$, strangeness $S = -1$ baryonic state around 1400 MeV. Integrated cross sections have been obtained for the $\pi\Sigma$ and $\bar{K}N$ channels, investigating the impact of unitarization in the results. The number of events with $\Lambda(1405)$ excitation in $\bar{\nu}_\mu p$ collisions in the recent antineutrino run at the MINER ν A experiment has also been obtained. We find that this reaction channel is relevant enough to be investigated experimentally and to be taken into account in the simulation models of future experiments with antineutrino beams.

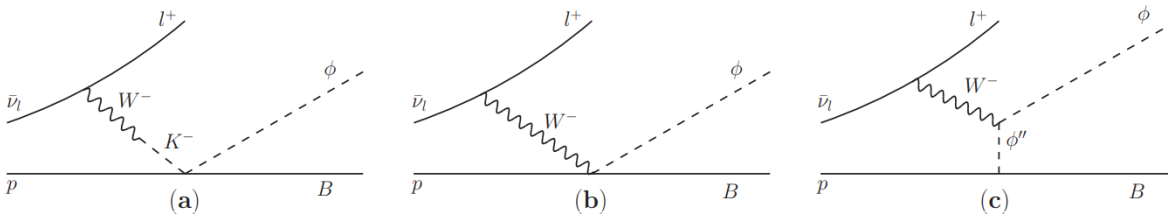


FIG. 1. Feynman diagrams for the process $\bar{\nu}_l p \rightarrow l^+ \phi B$. (a) denotes the kaon pole term (KP), (b) represents the contact term (CT), and (c) stands for the meson (ϕ'') in-flight term (MF).

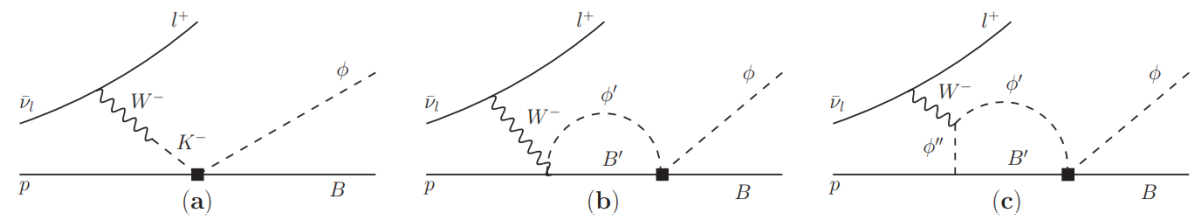


FIG. 2. Iterated loop diagrams for $\bar{\nu}_\mu p \rightarrow \mu^+ \phi B$. The solid boxes represent the T matrix of the ten coupled channels.

Evidence for Some New Hyperon Resonances -- to be Checked by K_L Beam Experiments

B.S. Zou (Beijing, Inst. Theor. Phys.) (Mar 12, 2016)

e-Print: 1603.03927 [hep-ph]

Various processes could be used to study these hyperon resonances. The neutrino induced hyperon production processes $\bar{\nu}_{e/\mu} + p \rightarrow e^+/\mu^+ + \pi + \Lambda/\Sigma$ may provide a unique clean place for studying low energy $\pi\Lambda/\Sigma$ interaction and hyperon resonances below KN threshold [36]. With plenty production of Λ_c at BESIII, JPARC, BelleII, $\Lambda_c^+ \rightarrow \pi^+\pi^0\Lambda$ could also be used to study Σ^* . The K^- , K_L beam experiments at JPARC and Jlab could provide an elegant new source for Λ^* , Σ^* and Ξ^{**} hyperon spectroscopy. $K_L p \rightarrow \Lambda\pi^+$, $\Sigma^0\pi^+$, $\Sigma^+\pi^0$, $\Sigma^{*0}\pi^+$, $\Sigma^{*+}\pi^0$ could pin down the $\Sigma^*(1540)3/2^-$; $K_L p \rightarrow \Sigma^0\pi^0\pi^+$, $\Lambda\pi^0\pi^+$ could shed light on the $\Sigma^*(1380 \sim 1500)1/2^-$, $\Sigma^*(1540)3/2^-$, $\Lambda^*(1680)3/2^+$; $K_L p \rightarrow \Sigma^0\eta\pi^+$, $\Lambda\eta\pi^+$ may check $\Sigma^*(1380 \sim 1500)1/2^-$, $\Sigma^*(1540)3/2^-$, $\Lambda^*(1670)3/2^-$. We believe the proposed K_L beam experiments at JLAB could settle down the spectrum of the low excited hyperon states which provide complimentary information to the study of penta-quark states with hidden charm [37, 38] and play a crucial role for understanding the hadron dynamics and hadron structure.

Summary

It looks various evidence for existence of $\Sigma(1/2-)$ around 1400 MeV, but not yet confirmed.



Thanks very much!



中国科学院大学
University of Chinese Academy of Sciences

